materials design

# WEBINAR

## VASP 6: Total energies beyond DFT

Martijn Marsman
University of Vienna, Austria

# Materials Design Webinar Series

- Share the webinar series with your colleagues!
  - Registration details

    http://www.materialsdesign.com/webinars
- We will be recording this webinar
  - Watch any of our earlier webinars anytime
  - We will post upcoming webinars on the webinar page
- Vote for the next webinar topic!
  - Take a 2 minutes brief survey at the end of the webinar!

# Please Ask Questions

full screen

during discussion:

Use the raise hand icon to bring attention to your question

any time during webinar: type your question here and then press Send

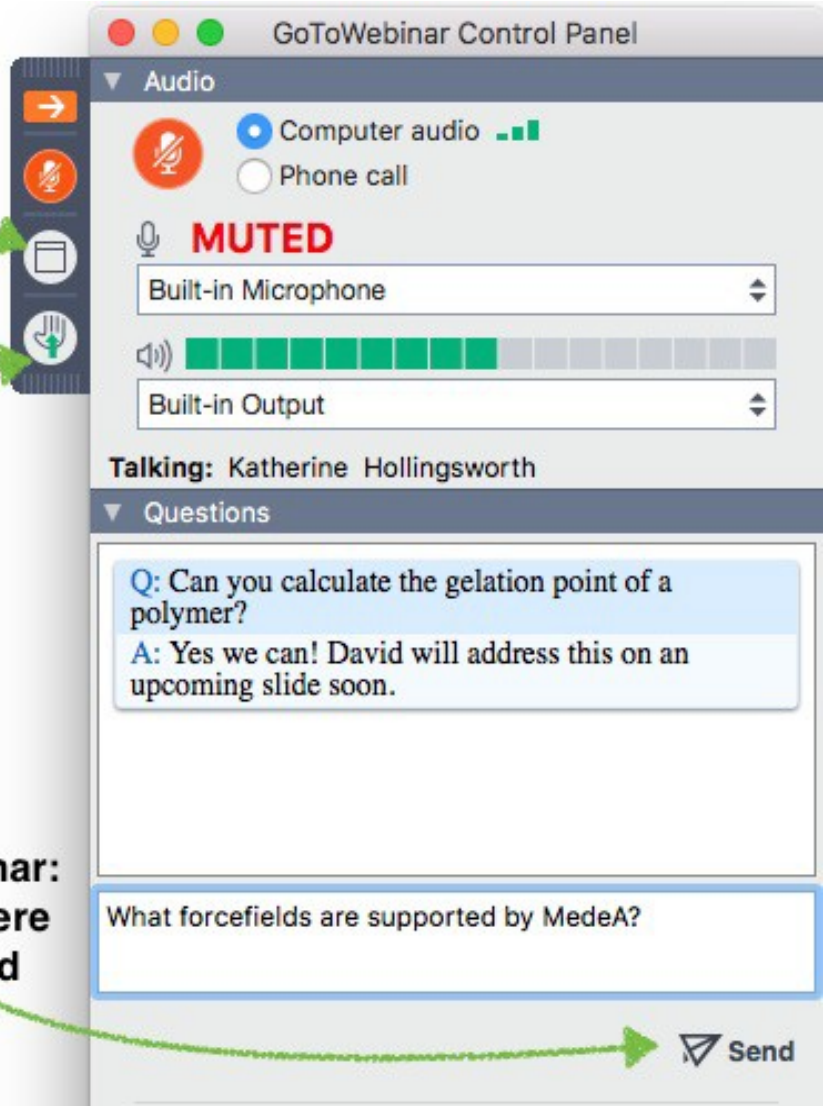

# Webinar Speakers


***Dr. Martijn Marsman***

*martijn.marsman@univie.ac.at*

***Katherine Hollingsworth***

*khollingsworth@materialsdesign.com*

# VASP6: total energies beyond DFT

Martijn Marsman

University Vienna & VASP Software GmbH


# Outline

- Beyond DFT
  - The need to go beyond DFT
  - HF/DFT hybrid functionals
  - The Random-Phase-Approximation
- $O(N^3)$ implementation of the RPA
  - Cubic-scaling RPA total energies
  - Minimax frequency and time integration
  - Cubic-scaling RPA quasi-particles
- Forces in the RPA

# Beyond DFT

Do we need to go beyond DFT?

# Catalysis: dehydrogenation of propane in Mordenite

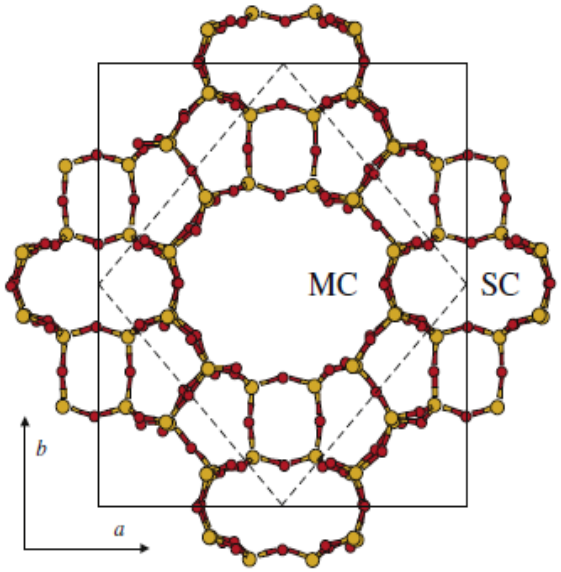


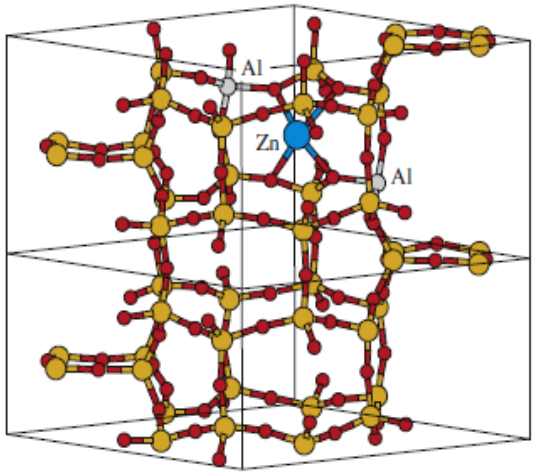


$$\mathrm{MOR{-}Zn} + \mathrm{C_3H_8} \rightarrow \mathrm{MOR{-}Zn \cdots C_3H_8},$$
$$\mathrm{MOR{-}Zn \cdots C_3H_8} \rightarrow \mathrm{H{-}MOR{-}Zn{-}C_3H_7},$$
$$\mathrm{H{-}MOR{-}Zn{-}C_3H_7} \rightarrow \mathrm{MOR{-}Zn \cdots C_3H_6} + \mathrm{H_2}$$
$$\mathrm{MOR{-}Zn \cdots C_3H_6} \rightarrow \mathrm{MOR{-}Zn} + \mathrm{C_3H_6}.$$

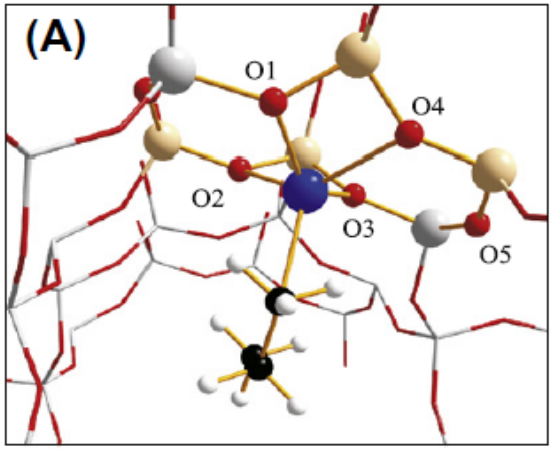


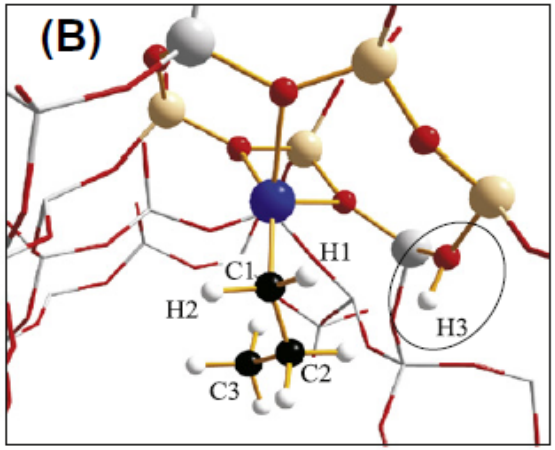


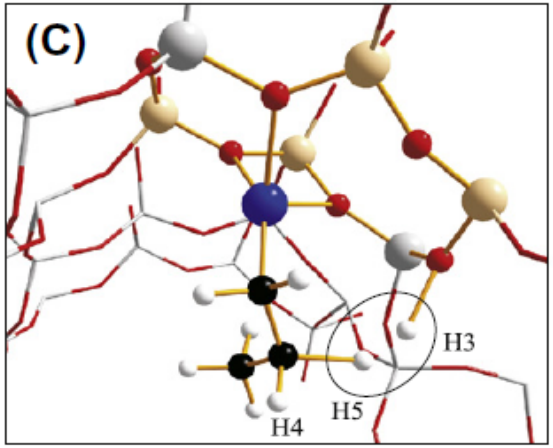


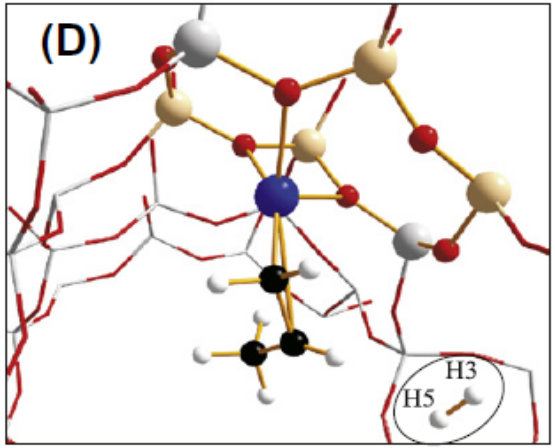


*L. Benco et al./Journal of Catalysis 277 (2011) 104–116*

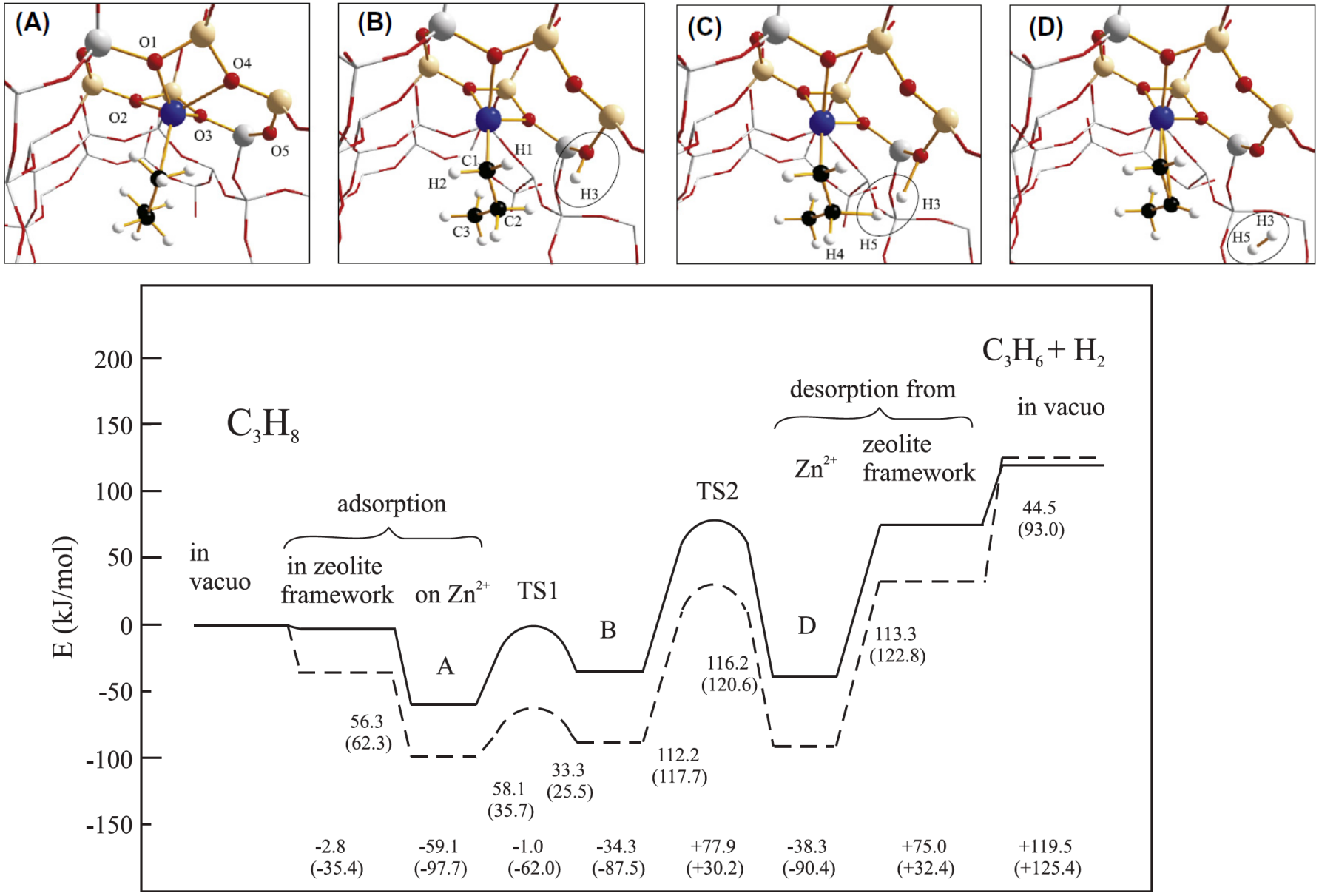


L. Benco *et al.*, Journal of Catalysis 227, 104 (2011)

# CO adsorption on d-metal surfaces

- DFT incorrectly predicts that CO prefers the hollow site: P. Feibelman *et al.*, J. Phys. Chem. B 105, 4018 (2001)
- This error is relatively large. Best DFT/PBE calculations:

| | |
|---|---|
| CO@Cu(111): | $-170$ meV |
| CO@Rh(111): | $-40$ meV |
| CO@Pt(111): | $-100$ meV |

- CO HOMO-LUMO gap too small in DFT:

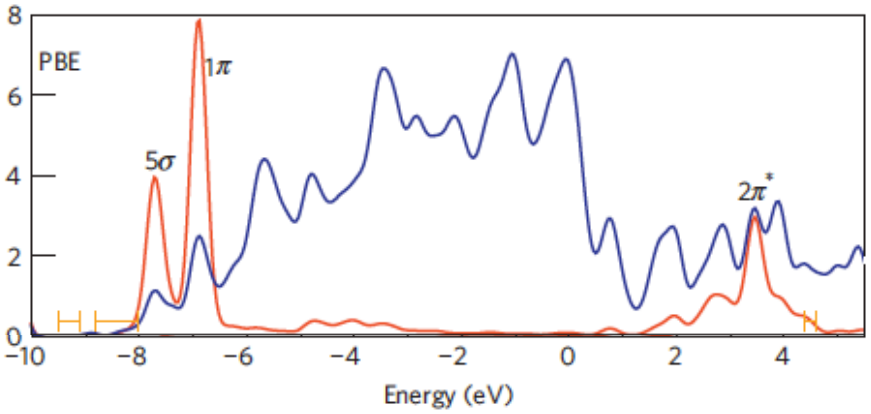


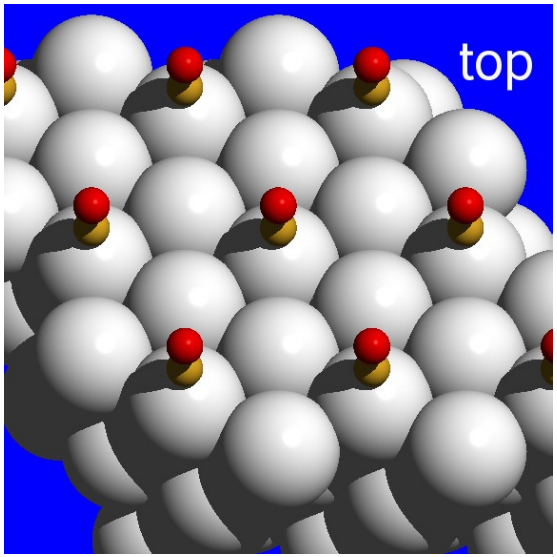


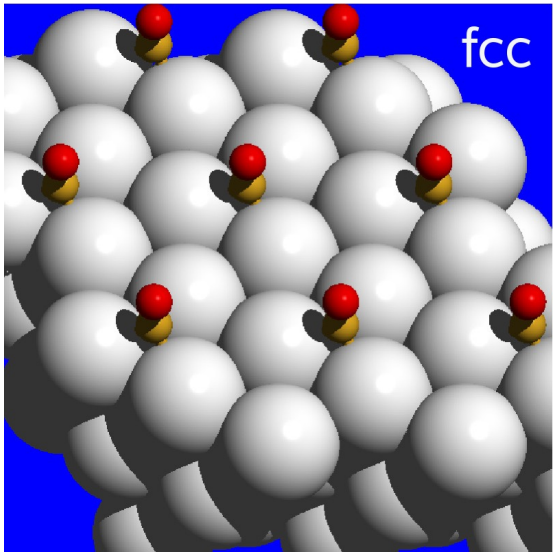

# Need to go beyond DFT?

Lattice constants and Bulk moduli:
AlP, AlAs, BAs, BP, Si, C, SiC, MgO, LiF

| | LDA | | PBE | | HF | |
|---|---|---|---|---|---|---|
| | $\Delta a_0$ | $\Delta B_0$ | $\Delta a_0$ | $\Delta B_0$ | $\Delta a_0$ | $\Delta B_0$ |
| MRE | -1.4 | 3.5 | 0.8 | -7.2 | 0.4 | 8.2 |
| MARE | 1.4 | 7.9 | 0.8 | 7.2 | 0.7 | 8.2 |

(All in %)

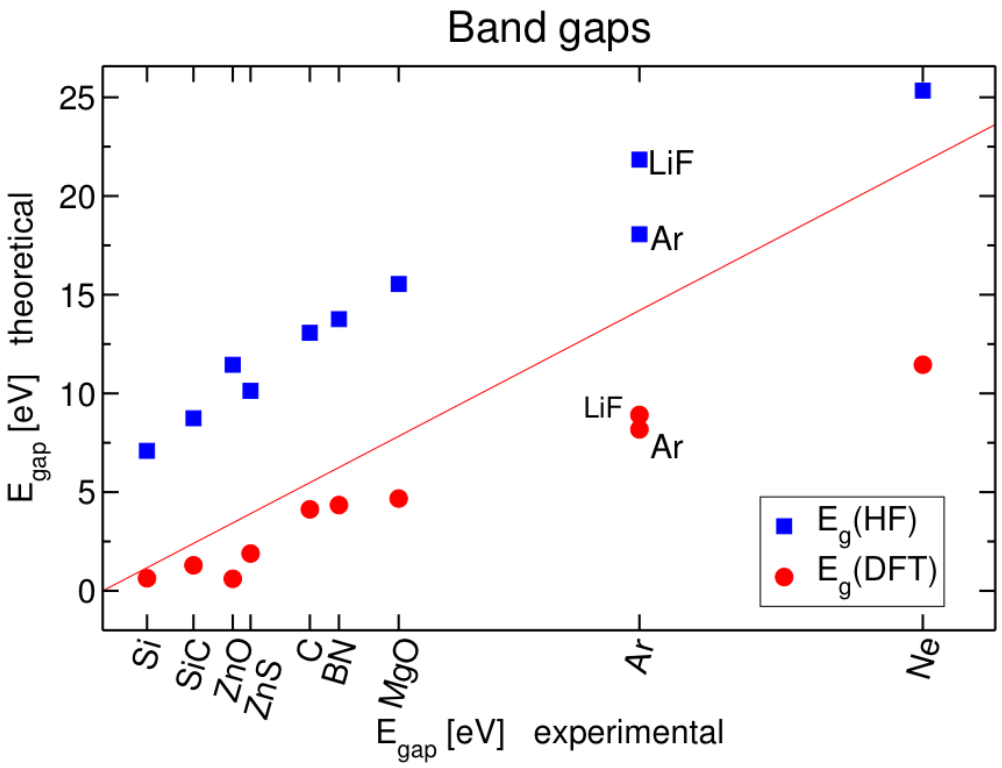


| ΔH (kJ/mol) | PBE | EXP |
|---|---|---|
| $Al+N_2 \rightarrow AlN$ | 262 | 350 |
| $Mg+H_2 \rightarrow MgH_2$ | 52 | 78 |
| Si+C→SiC | 51 | 69 |
| CO→CO@Rh | 183 | 144 |

(More) accurate treatment of electronic correlation needed for, e.g:

- Band gaps (optical properties)
- Total energy differences with ”chemical accuracy” (1 kcal/mol ≈ 40 meV): Atomization-, formation energies, reaction barriers, *etc*
- Van der Waals interactions

# Hybrid functionals

Hartree-Fock-DFT hybrid:

$$E_{\mathrm{xc}}^{\mathrm{hyb.}} = aE_X^{\mathrm{HF}} + (1-a)E_X^{\mathrm{DFT}} + E_c^{\mathrm{DFT}}$$

where

$$E_x^{\mathrm{HF}} \propto \sum_{i,j}^{\mathrm{occ.}} \int\int d^3\mathbf{r} d^3\mathbf{r}' \frac{\psi_i^*(\mathbf{r})\psi_j(\mathbf{r})\psi_j^*(\mathbf{r}')\psi_i(\mathbf{r}')}{|\mathbf{r}-\mathbf{r}'|}$$

Solve a one-electron (Roothaan) equation:

$$\left(-\frac{1}{2}\Delta + V_{\mathrm{ext}}(\mathbf{r}) + V_{\mathrm{H}}(\mathbf{r}) + \right)\psi_i(\mathbf{r}) + \int V_{\mathrm{X}}(\mathbf{r},\mathbf{r}')\psi_i(\mathbf{r}')d\mathbf{r}' = \epsilon_i\psi_i(\mathbf{r})$$

with an orbital dependent, non-local potential (compare to DFT)

$$V_X(\mathbf{r},\mathbf{r}') = -\sum_j^{\mathrm{occ.}} \frac{\psi_j(\mathbf{r})\psi_j^*(\mathbf{r}')}{|\mathbf{r}-\mathbf{r}'|} \qquad V_{\mathrm{xc}}[\rho](\mathbf{r})\psi_i(\mathbf{r})$$

# Hybrid functionals

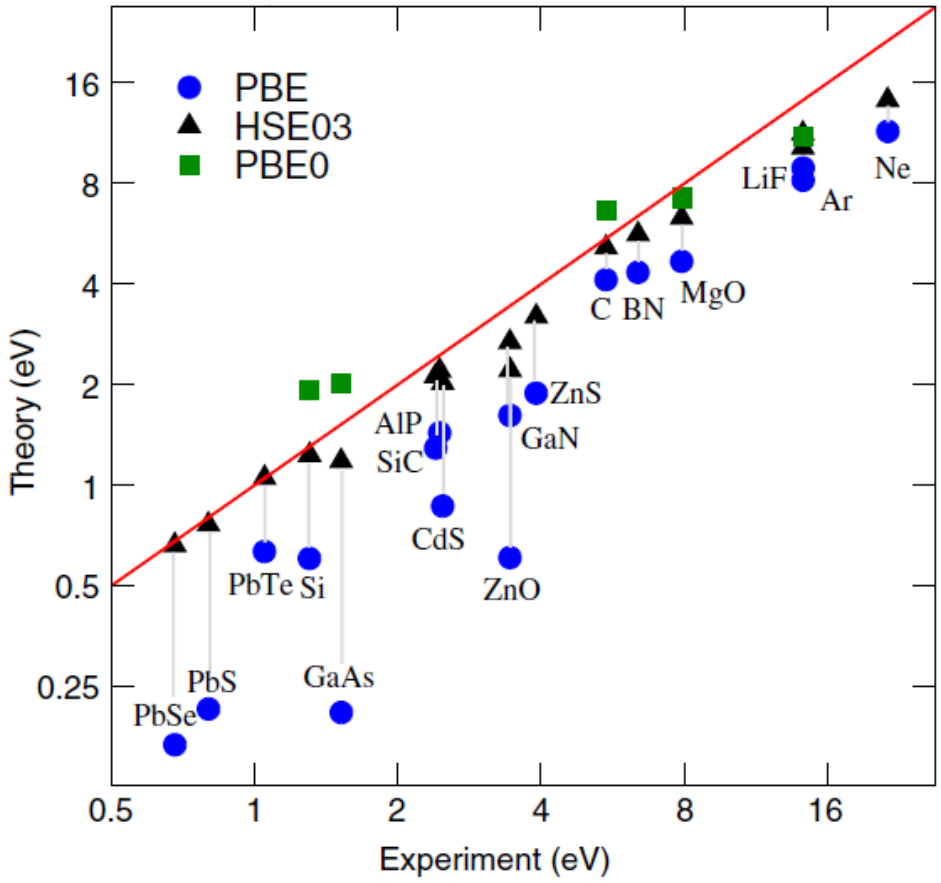


**Figure 8.** Band gaps from PBE, PBE0, and HSE03 calculations, plotted against data from experiment.

Lattice constant

| | MRE | MARE |
|---|---|---|
| PBE | 0.8 | 1.0 |
| PBE0 | 0.1 | 0.5 |
| HSE | 0.2 | 0.5 |
| B3LYP | 1.0 | 1.2 |

Bulk modulus

| | MRE | MARE |
|---|---|---|
| PBE | -9.8 | 9.4 |
| PBE0 | -1.2 | 5.7 |
| HSE | -3.1 | 6.4 |
| B3LYP | -10.2 | 11.4 |

Atomization energy

| | MRE | MARE |
|---|---|---|
| PBE | -1.9 | 3.4 |
| PBE0 | -6.5 | 7.4 |
| HSE | -5.1 | 6.3 |
| B3LYP | -17.6 | 17.6 |

(All in %)

# CO adsorption on d-metal surfaces

| CO @ | | top | fcc | hcp | $\Delta$ |
|---|---|---|---|---|---|
| Cu(111) | PBE | 0.709 | 0.874 | 0.862 | −0.165 |
| | PBE0 | 0.606 | 0.579 | 0.565 | 0.027 |
| | HSE03 | 0.561 | 0.555 | 0.535 | 0.006 |
| | exp. | 0.46-0.52 | | | |
| Rh(111) | PBE | 1.870 | 1.906 | 1.969 | −0.099 |
| | PBE0 | 2.109 | 2.024 | 2.104 | 0.005 |
| | HSE03 | 2.012 | 1.913 | 1.996 | 0.016 |
| | exp. | 1.43-1.65 | | | |
| Pt(111) | PBE | 1.659 | 1.816 | 1.750 | −0.157 |
| | PBE0 | 1.941 | 1.997 | 1.944 | −0.056 |
| | HSE03 | 1.793 | 1.862 | 1.808 | −0.069 |
| | exp. | 1.43-1.71 | | | |

(All energies in eV)

A. Stroppa *et al.*, PRB 76, 195440 (2007); A. Stroppa and G. Kresse, NJP 10, 063020 (2008).

## Hybrid functionals reduce the tendency to stabilize adsorption at the hollow site w.r.t. the top site.

## reduced CO $2\pi^*$ – metal-*d* interaction

- DFT does well for the metallic surface, but not for the CO: $2\pi^*$ (LUMO) too close to the Fermi level.
- HSE does well for the CO, but not for the surface: *d*-metal bandwidth too large.

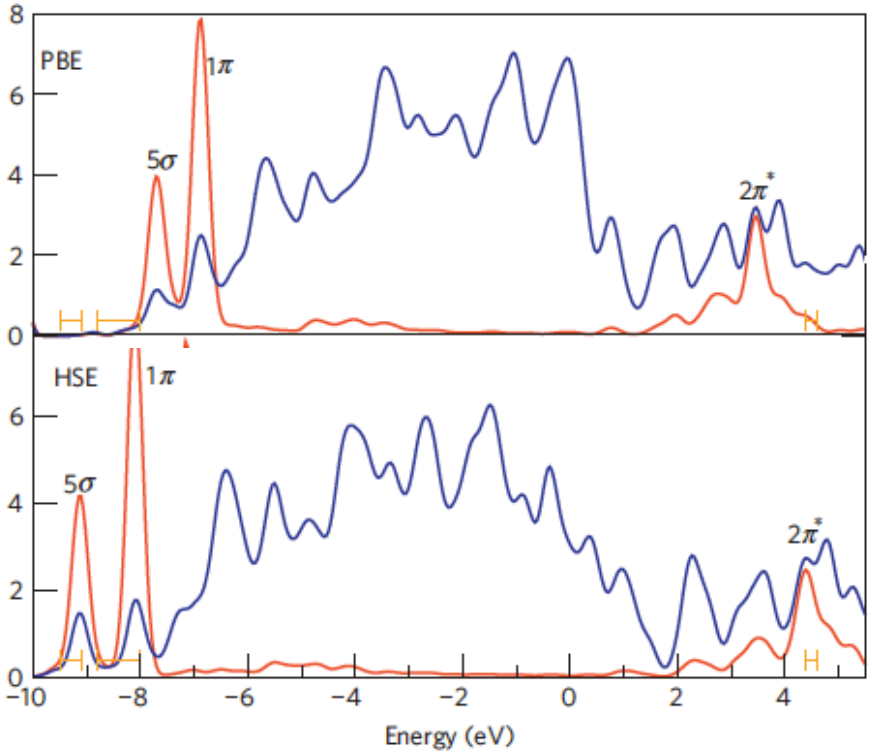


Schimka et al., Nature Materials 9, 741 (2010)

# Need to go beyond DFT and DFT/HF hybrids?

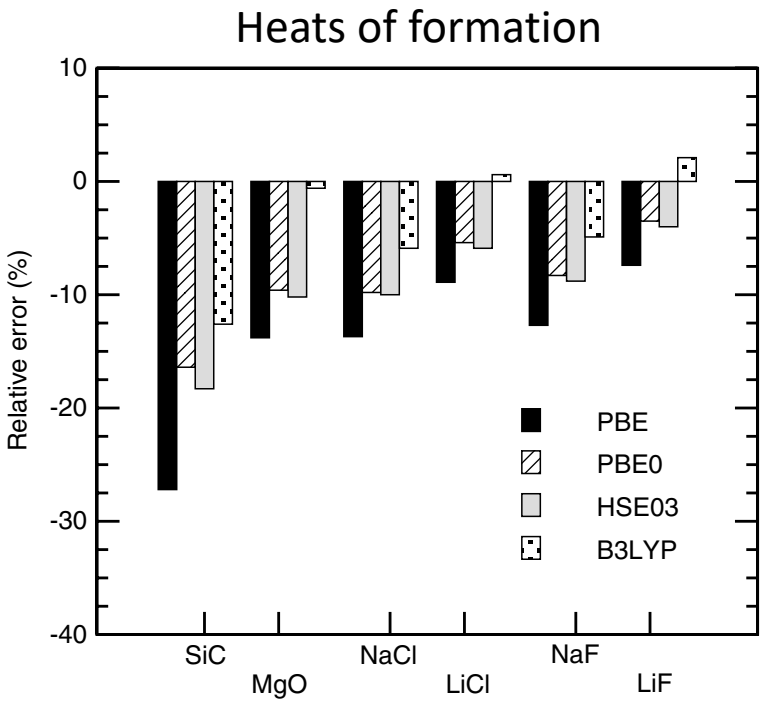


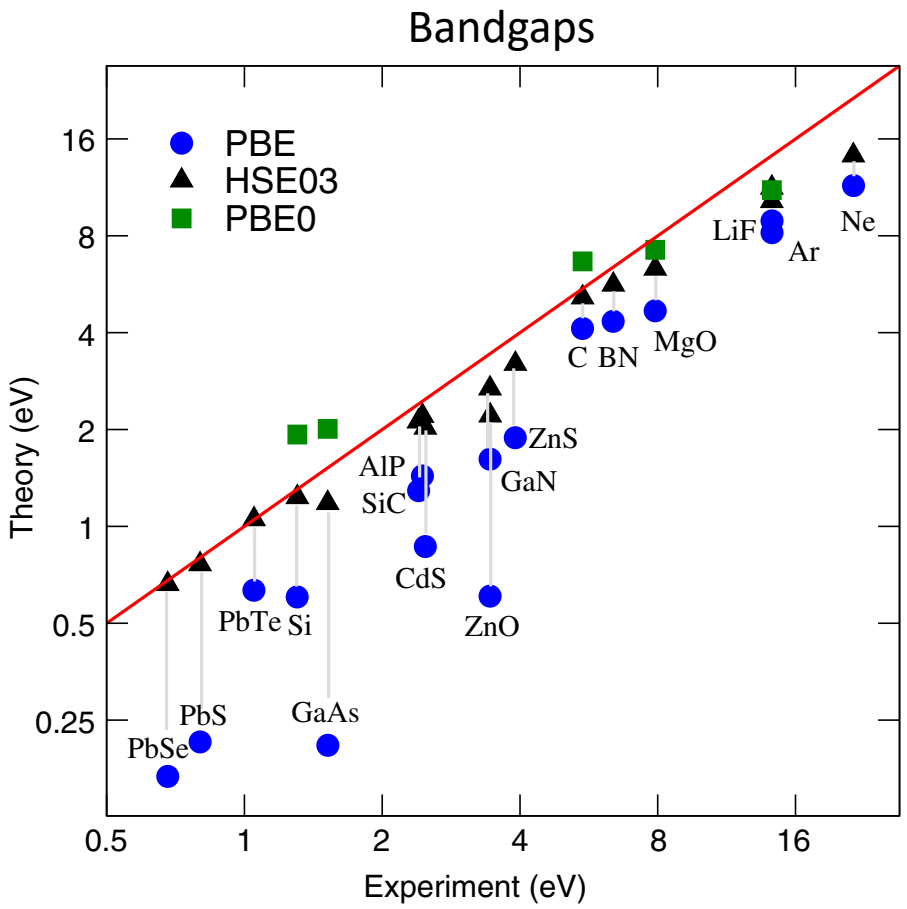


- Total energy differences with ”chemical accuracy” (1 kcal/mol ≈ 40 meV/atom): Atomization-, formation energies, reaction barriers, *etc*
- Van der Waals interactions

- Bandstructure of metals and *largish* gap systems, and some problematic cases inbetween

# The Random-Phase-Approximation: GW and ACFDT

# One-electron/QP picture

DFT: Kohn-Sham eq.

$$\left(-\frac{1}{2}\Delta + V_{\mathrm{ext}}(\mathbf{r}) + V_{\mathrm{H}}(\mathbf{r}) + V_{\mathrm{xc}}\left[\rho\right](\mathbf{r})\right)\psi_{n\mathbf{k}}(\mathbf{r}) = \epsilon_{n\mathbf{k}}\psi_{n\mathbf{k}}(\mathbf{r})$$

DFT-HF hybrid functionals: Roothaan eq.

$$\left(-\frac{1}{2}\Delta + V_{\mathrm{ext}}(\mathbf{r}) + V_{\mathrm{H}}(\mathbf{r})\right)\psi_{n\mathbf{k}}(\mathbf{r}) + \int V_{\mathrm{X}}\left[\{\psi_o\}\right](\mathbf{r},\mathbf{r}')\psi_{n\mathbf{k}}(\mathbf{r}')d\mathbf{r}' = \epsilon_{n\mathbf{k}}\psi_{n\mathbf{k}}(\mathbf{r})$$

GW: quasi-particle eq.

$$\left(-\frac{1}{2}\Delta + V_{\mathrm{ext}}(\mathbf{r}) + V_{\mathrm{H}}(\mathbf{r})\right)\psi_{n\mathbf{k}}(\mathbf{r}) + \int \Sigma\left[\{\psi, E\}\right](\mathbf{r},\mathbf{r}', E_{n\mathbf{k}})\psi_{n\mathbf{k}}(\mathbf{r}')d\mathbf{r}' = E_{n\mathbf{k}}\psi_{n\mathbf{k}}(\mathbf{r})$$

# GW

The quasi-particle equation:

$$\left(-\frac{1}{2}\Delta + V_{\text{ext}}(\mathbf{r}) + V_{\text{H}}(\mathbf{r})\right)\psi_{n\mathbf{k}}(\mathbf{r}) + \int \Sigma(\mathbf{r},\mathbf{r}',E_{n\mathbf{k}})\psi_{n\mathbf{k}}(\mathbf{r}')d\mathbf{r}' = E_{n\mathbf{k}}\psi_{n\mathbf{k}}(\mathbf{r})$$

The "self-energy is given by: $\Sigma = iGW$

Green's function: G

or more explicitly

$$\Sigma(\mathbf{r},\mathbf{r}',E) = \frac{i}{2\pi}\int_{-\infty}^{\infty} d\omega \sum_{n}^{\text{all}} \frac{\psi_n(\mathbf{r})\psi_n^*(\mathbf{r}')}{\omega - E - E_n + i\eta\,\text{sgn}(E_n - E_{\text{fermi}})} \times$$

$$\times\, e^2 \int d\mathbf{r}'' \frac{\epsilon^{-1}(\mathbf{r},\mathbf{r}'',\omega)}{|\mathbf{r}'' - \mathbf{r}'|}$$

screened Coulomb interaction: W

Compare to Fock-exchange:

$$V_{\text{X}}(\mathbf{r},\mathbf{r}') = -\sum_{n}^{\text{occ.}} \psi_n(\mathbf{r})\psi_n^*(\mathbf{r}') \times \frac{e^2}{|\mathbf{r} - \mathbf{r}'|}$$

bare Coulomb interaction: *v*

# The Green's function: physical interpretation

The Green's function $G(\mathbf{r}, \mathbf{r}', t - t')$ describes the propagation of a particle from $(\mathbf{r}, t)$ to $(\mathbf{r}', t')$: i.e., provided we have particle at position **r** at time *t*, $G(\mathbf{r}, \mathbf{r}', t - t')$ is the chance of finding it at position **r**' at time *t*'.

$$G_0(\mathbf{r}, \mathbf{r}', \omega) = \sum_n^{\text{all}} \frac{\psi_n^*(\mathbf{r})\psi_n(\mathbf{r}')}{\omega - \epsilon_n + i\eta \, \text{sgn}(\epsilon_n - \mu)}$$

- Particle propagator: $G_o(1,2) = G_o(\mathbf{r}_1, \mathbf{r}_2, t_2 - t_1)$ for $t_2 > t_1$:

$(\mathbf{r}_1, t_1) = 1$ $\qquad$ $(\mathbf{r}_2, t_2) = 2$

$$G_0(1,2) = \sum_n^{\text{vir.}} \psi_n(\mathbf{r}_1)^* \psi_n(\mathbf{r}_2) e^{-i(\epsilon_n - \mu)(t_2 - t_1)}$$

- Hole propagator: $G_o(1,2)$ for $t_1 > t_2$:

$(\mathbf{r}_2, t_2) = 2$ $\qquad$ $(\mathbf{r}_1, t_1) = 1$

$$G_0(1,2) = \sum_n^{\text{occ.}} \psi_n^*(\mathbf{r}_1)\psi_n(\mathbf{r}_2) e^{-i(\epsilon_n - \mu)(t_1 - t_2)}$$

# W in the Random-Phase-Approximation

Key: the "irreducible polarizability in the independent particle picture" $\chi^0$ (or $\chi^{\mathrm{KS}}$):

$$\chi^0(\mathbf{r},\mathbf{r}',\omega) := \frac{\partial \rho_{\mathrm{ind}}(\mathbf{r},\omega)}{\partial v_{\mathrm{eff}}(\mathbf{r}',\omega)}$$

In the RPA, the screened Coulomb interaction is computed from $\chi^0$ as:

$$W = \nu + \nu\chi_0\nu + \nu\chi_0\nu\chi_0\nu + \nu\chi_0\nu\chi_0\nu\chi_0\nu + \ldots = \nu\underbrace{(1-\chi_0\nu)^{-1}}_{\epsilon^{-1}}$$

geometrical series

1. The bare Coulomb interaction between two particles

2. The electronic environment reacts to the field generated by a particle: induced change in the density $\chi_0 v$, that gives rise to a change in the Hartree potential: $v\chi_0 v$.

3. The electrons react to the induced change in the potential: additional change in the density, $\chi_0 v\chi_0 v$, and corresponding change in the Hartree potential: $v\chi_0 v\chi_0 v$.

and so on, and so on …

$$W = \epsilon^{-1}\nu \qquad \epsilon^{-1} = 1 + \nu\chi \qquad \chi = \chi^0 + \chi^0\nu\chi$$

# The IP-polarizability: $\chi_0$

The "irreducible polarizability in the independent particle picture" $\chi^0$ (or $\chi^{\mathrm{KS}}$):

$$\chi^0(\mathbf{r},\mathbf{r}',\omega) := \frac{\partial \rho_{\mathrm{ind}}(\mathbf{r},\omega)}{\partial v_{\mathrm{eff}}(\mathbf{r}',\omega)}$$

Adler and Wiser derived expressions for $\chi^0$

$$\chi_0(\mathbf{r}_1,\mathbf{r}_2,\omega) = \sum_i^{\text{occ.}} \sum_a^{\text{virt.}} \frac{\langle\psi_a|\mathbf{r}_1|\psi_i\rangle\langle\psi_i|\mathbf{r}_2|\psi_a\rangle}{\epsilon_i - \epsilon_a - \omega} + \sum_i^{\text{occ.}} \sum_a^{\text{virt.}} \frac{\langle\psi_i|\mathbf{r}_1|\psi_a\rangle\langle\psi_a|\mathbf{r}_2|\psi_i\rangle}{\epsilon_a - \epsilon_i - \omega}$$

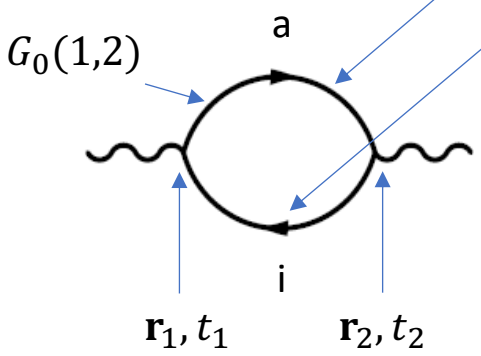


Or in terms of Green's functions (propagators):

$$\chi_0(\mathbf{r}_1,t_1,\mathbf{r}_2,t_2) = \chi(1,2) = -G_0(1,2)G_0(2,1)$$

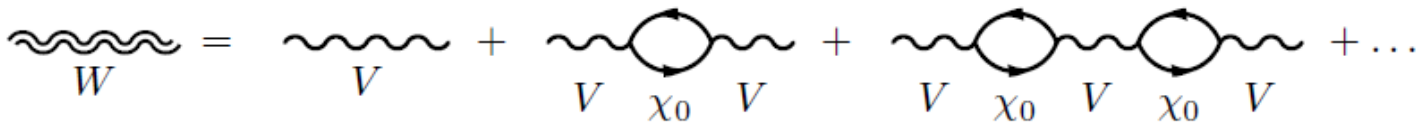

# GW in the RPA

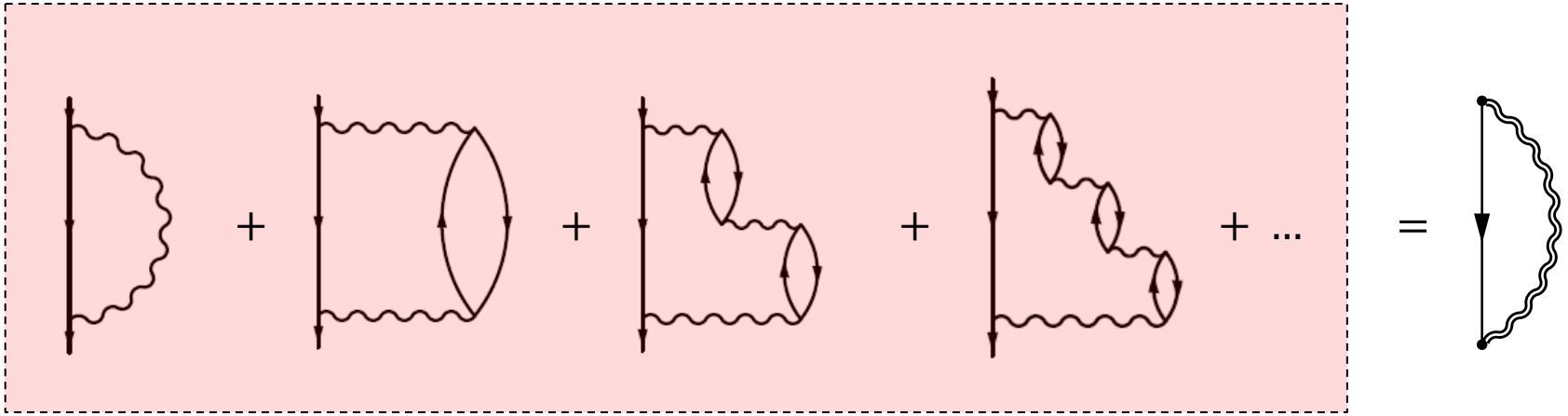

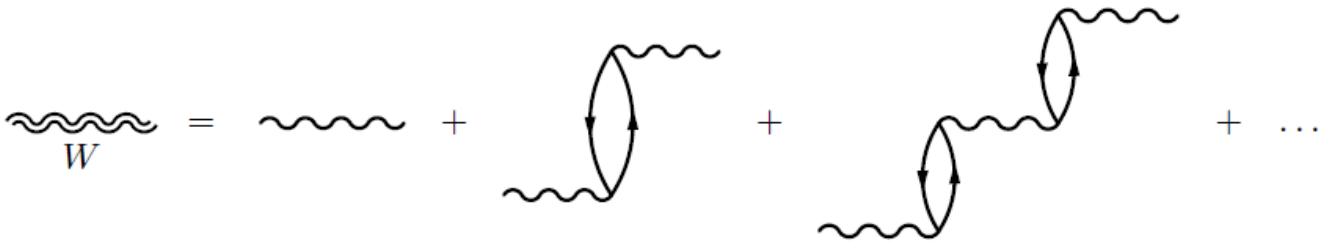


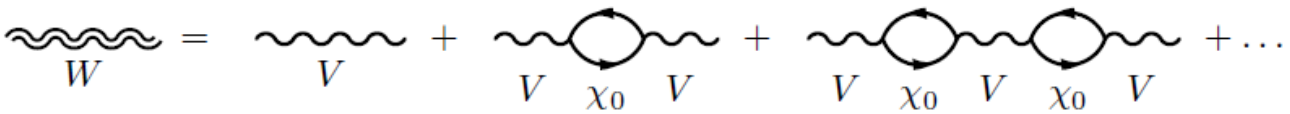

# RPA total energies (ACFDT)

The "RPA" total energy is given by:

$$E[n] = T_{KS}[\{\psi_i\}] + E_H[n] + E_X[\{\psi_i\}] + E_{\mathrm{ion-el}}[n] + E_c$$

with the RPA correlation energy

$$E_c = \sum_{\mathbf{q}} \int_0^\infty \frac{d\omega}{2\pi} \mathrm{Tr}\{\ln[1 - \chi_0(\mathbf{q}, i\omega)\nu] + \chi_0(\mathbf{q}, i\omega)\nu\}$$

and the Independent-Particle polarizability: $\chi^0(\mathbf{r}, \mathbf{r}', \omega) := \frac{\partial \rho_{\mathrm{ind}}(\mathbf{r}, \omega)}{\partial v_{\mathrm{eff}}(\mathbf{r}', \omega)}$

$$\chi^0_{\mathbf{G},\mathbf{G}'}(\mathbf{q}, \omega) = \frac{1}{\Omega} \sum_{nn'\mathbf{k}} 2w_{\mathbf{k}}(f_{n'\mathbf{k}+\mathbf{q}} - f_{n'\mathbf{k}}) \times \frac{\langle \psi_{n'\mathbf{k}+\mathbf{q}} | e^{i(\mathbf{q}+\mathbf{G})\mathbf{r}} | \psi_{n\mathbf{k}} \rangle \langle \psi_{n\mathbf{k}} | e^{-i(\mathbf{q}+\mathbf{G}')\mathbf{r}'} | \psi_{n'\mathbf{k}+\mathbf{q}} \rangle}{\epsilon_{n'\mathbf{k}+\mathbf{q}} - \epsilon_{n\mathbf{k}} - \omega - i\eta}$$

$$\ln(1 - \chi_0 v) + \chi_0 v = -\frac{\mathrm{Tr}[\chi_0 v \chi_0 v]}{2} - \frac{\mathrm{Tr}[\chi_0 v \chi_0 v \chi_0 v]}{3} - \frac{\mathrm{Tr}[\chi_0 v \chi_0 v \chi_0 v \chi_0 v]}{4} \ldots$$

# In terms of diagrams

$$\ln(1-\chi_0 v)+\chi_0 v = -\frac{\mathrm{Tr}[\chi_0 v \chi_0 v]}{2} - \frac{\mathrm{Tr}[\chi_0 v \chi_0 v \chi_0 v]}{3} - \frac{\mathrm{Tr}[\chi_0 v \chi_0 v \chi_0 v \chi_0 v]}{4}$$

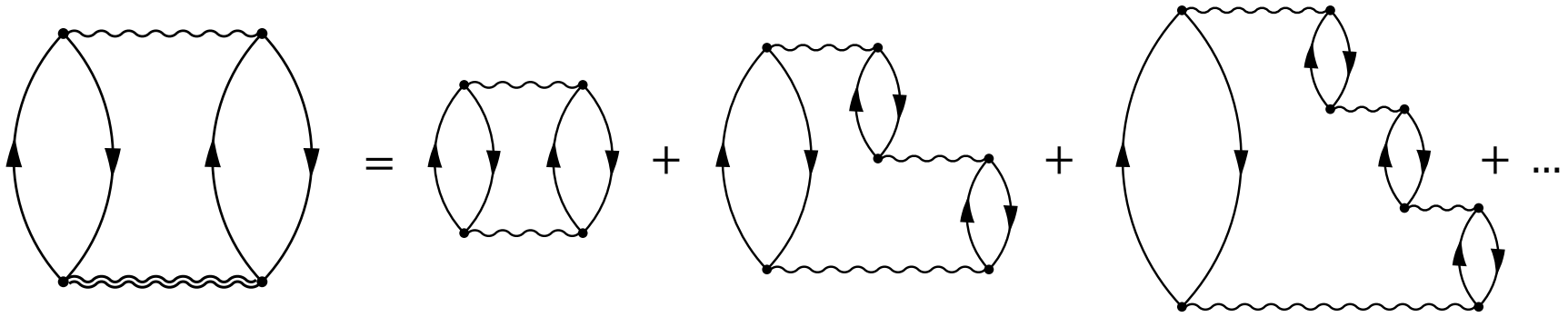

2nd. order 3rd. order 4th. order

The derivate w.r.t. *G* yields GW!

$$\frac{\partial E_c}{\partial G} = \Sigma$$

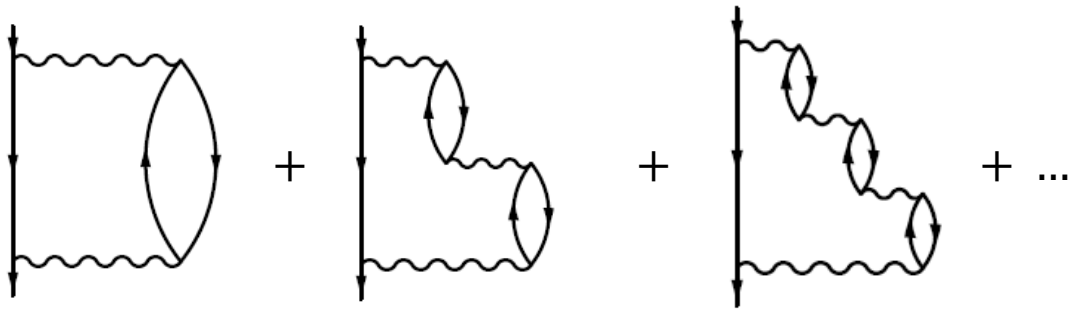

# RPA: lattice constants

J. Harl et al., PRB 81, 115126 (2010)

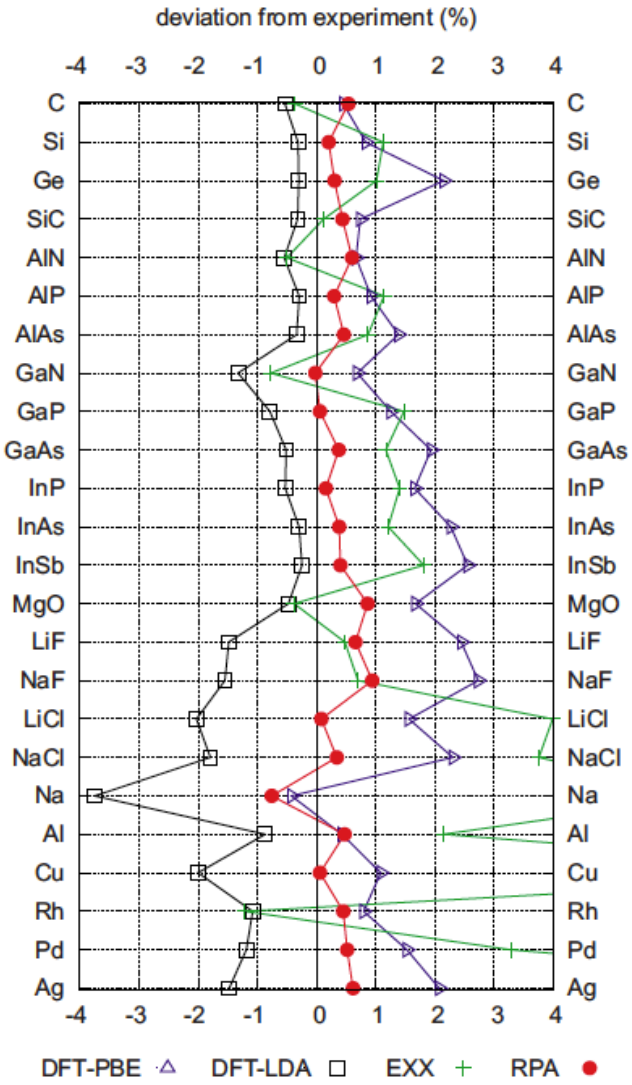


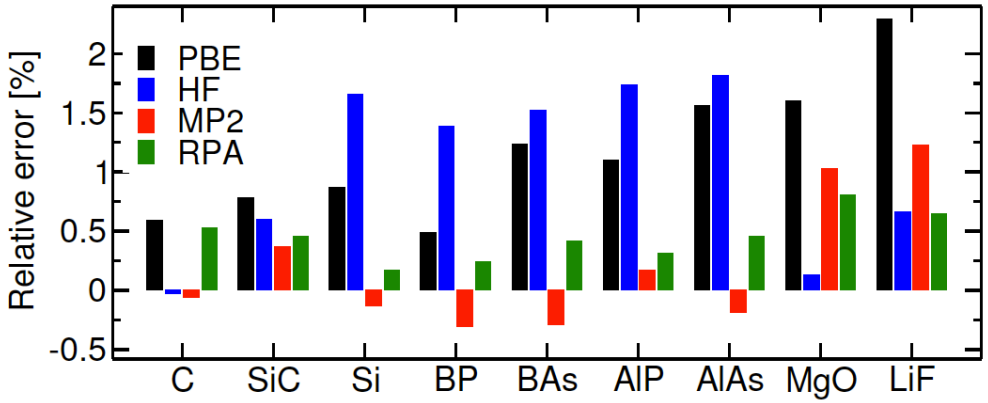


Deviations w.r.t. experiment
(corrected for zero-point vibrations)

| | MRE | MARE |
|---|---|---|
| PBE | 1.2 | 1.2 |
| HF | 1.1 | 1.1 |
| MP2 | 0.2 | 0.4 |
| RPA | 0.5 | 0.4 |

(in %)

# RPA: noble gas solids

J. Harl and G. Kresse, PRB 77, 045136 (2008)

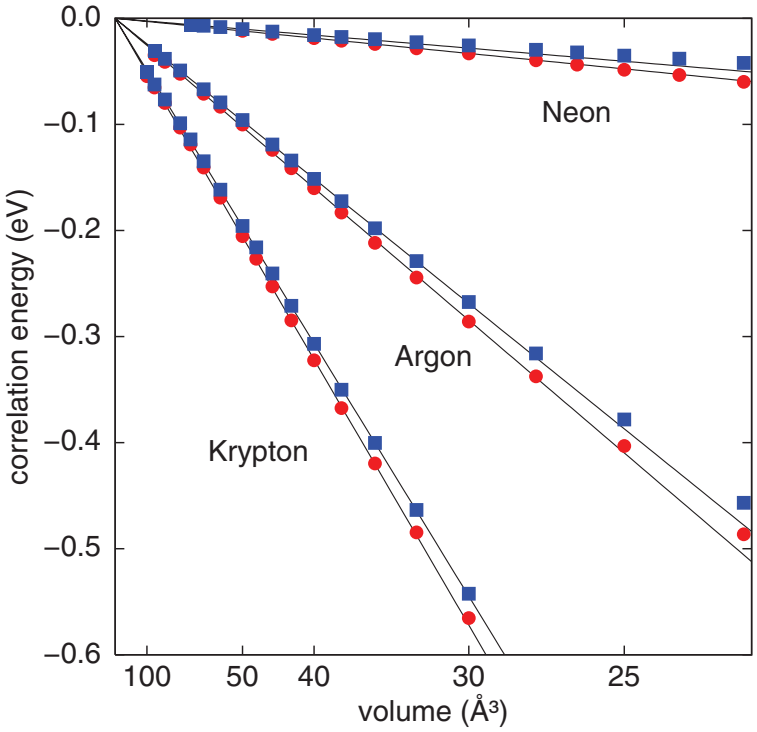


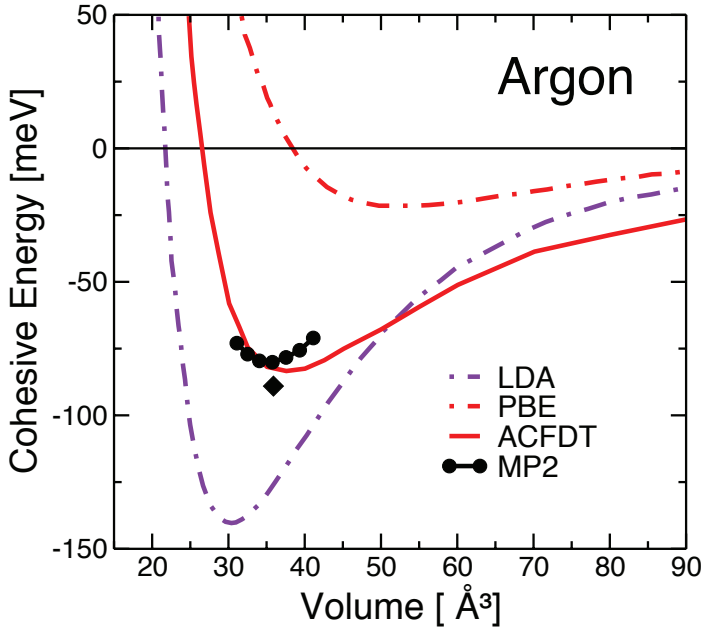


$C_6$ coefficients

| | RPA(LDA) | RPA(PBE) | Exp. |
|---|---|---|---|
| Ne | 62 | 53 | 47 |
| Ar | 512 | 484 | 455 |
| Kr | 1030 | 980 | 895 |

# Graphite vs. Diamond

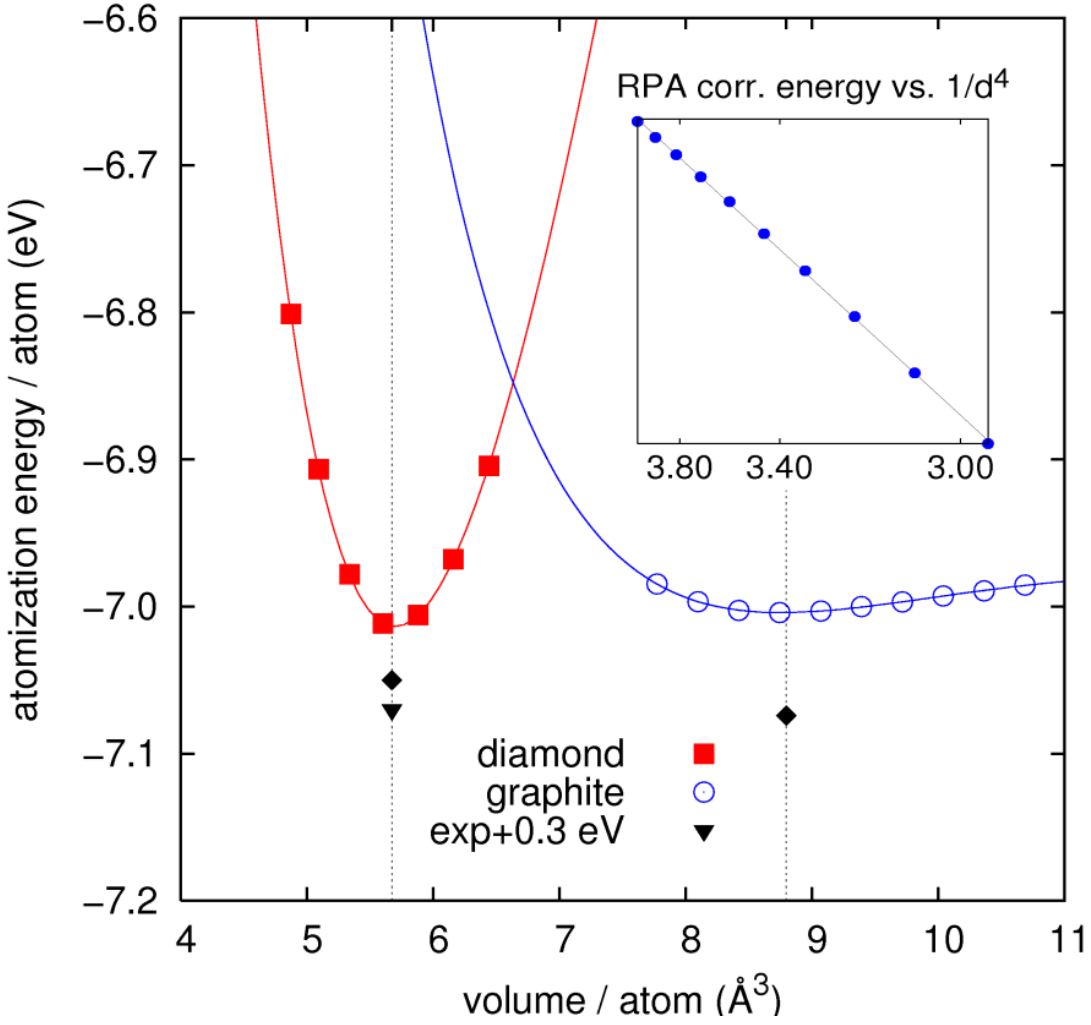


$1/d^4$ behavior at short distances

| | QMC (Galli) | RPA | EXP |
|---|---|---|---|
| d(Å) | 3.426 | 3.34 | 3.34 |
| $C_{33}$ | | 36 | 36-40 |
| E(meV) | 56 | 48 | 43-50 |

J. Harl, G. Kresse,
PRL 103, 056401 (2009).
S. Lebeque, et al.,
PRL 105, 196401 (2010).

# RPA: heats of formation

J. Harl and G. Kresse, PRL 103, 056401 (2009)

Heats of formation w.r.t. normal state at ambient conditions (in kJ/mol)

Example: Mg(bulk metal) + $H_2 \rightarrow MgH_2$

| | PBE | Hartree-Fock | RPA | EXP |
|---|---|---|---|---|
| LiF | 570 | 664 | 609 | 621 |
| NaF | 522 | 607 | 567 | 576 |
| NaCl | 355 | 433 | 405 | 413 |
| MgO | 516 | 587 | 577 | 603 |
| $MgH_2$ | 52 | 113 | 72 | 78 |
| AlN | 262 | 350 | 291 | 321 |
| SiC | 51 | 69 | 64 | 69 |

# RPA: CO @ Pt(111) and Rh(111)

Schimka et al., Nature Materials 9, 741 (2010)

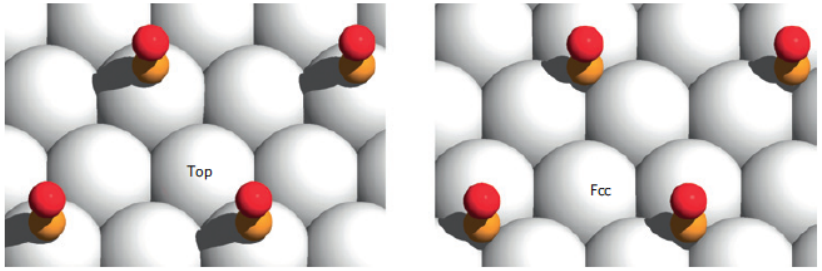


RPA:

- increases surface energy and
- decreases adsorption energy

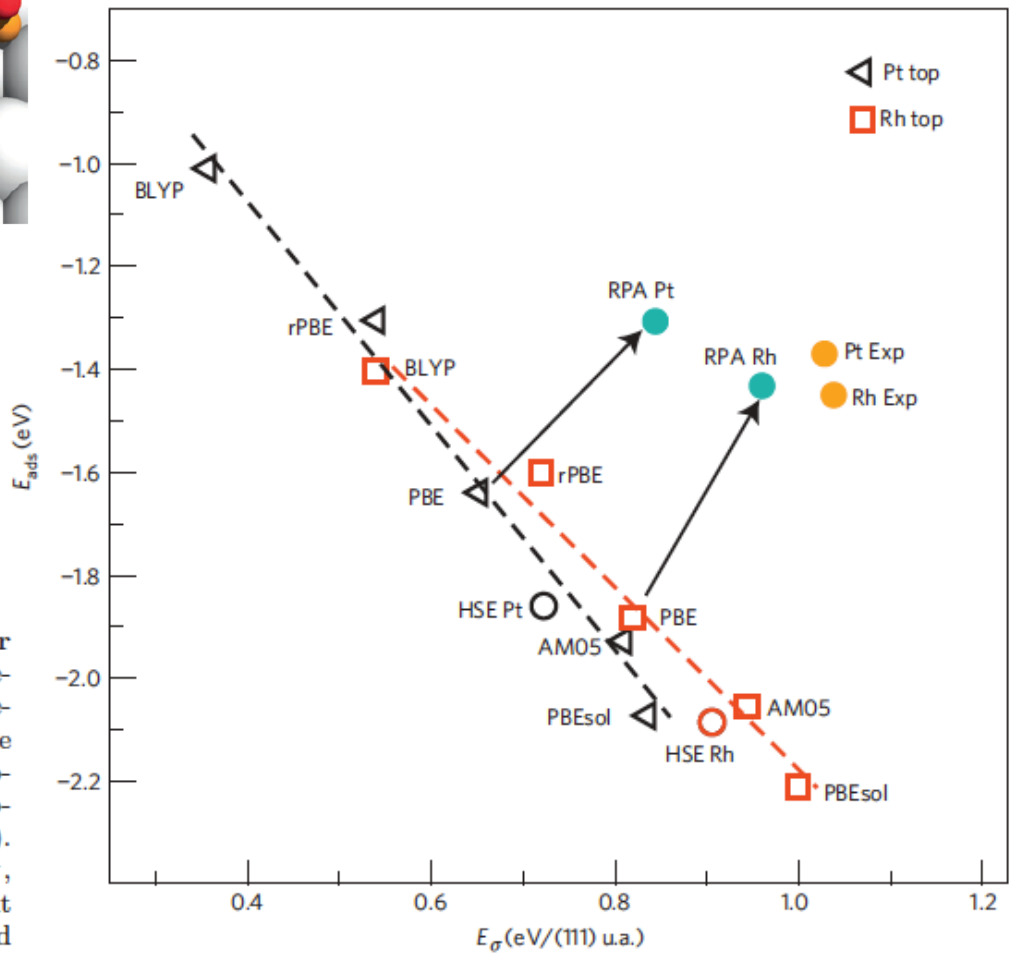


FIG. 1: **Atop CO adsorption and surface energies for Pt(111) and Rh(111).** (a) Considered CO adsorption geometries for a $(2 \times 2)$ surface cell. Semi-local functionals predict CO to adsorb in the fcc hollow site coordinated to three metal atoms on Pt and Rh, whereas experiments unequivocally show adsorption atop a metal atom. (b) Atop adsorption energies versus surface energies for Pt(111) and Rh(111). Various semi-local functionals were used: AM05[10], PBEsol[11], PBE[8], rPBE[12] and BLYP[13], in order of increasing gradient corrections. Furthermore the hybrid functional HSE[18] based on the PBE functional was used.

- DFT does well for the metallic surface, but not for the CO: $2\pi^*$ (LUMO) too close to the Fermi level.
- HSE does well for the CO, but not for the surface: *d*-metal bandwith too large.
- GW gives a good description of both the metallic surface as well as of the CO $2\pi^*$ (LUMO). The CO $5\sigma$ and $1\pi$ are slightly underbound.

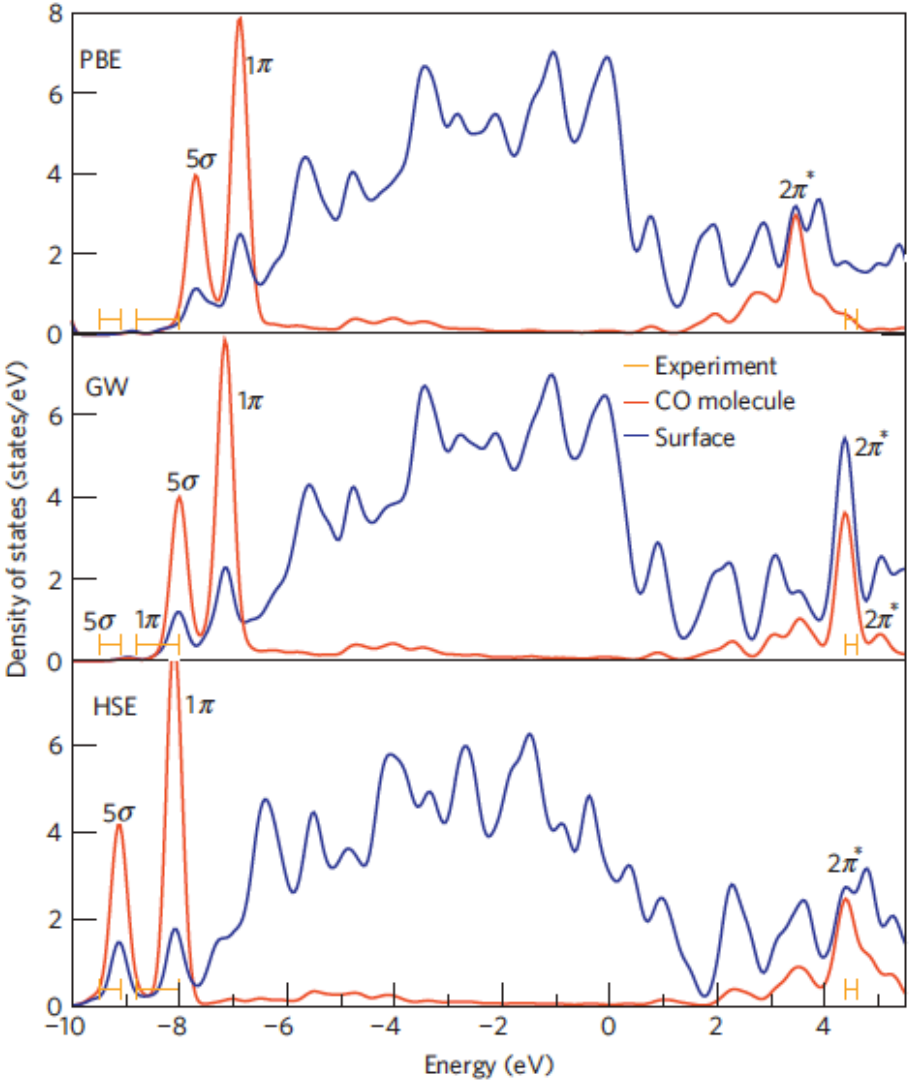


**Figure 2 | Electronic DOS for CO adsorbed atop a Pt atom on Pt(111).** The DOS is evaluated using DFT (PBE), the RPA (GW) and a hybrid functional (HSE). Experimental photoemission data for the $2\pi^*$ state are from ref. 19, for the $5\sigma$ and $1\pi$ state from ref. 20.

Schimka et al., Nature Materials 9, 741 (2010)

RPA:

- Right site preference
- Good adsorption energies
- Excellent lattice constants
- Good surface energies

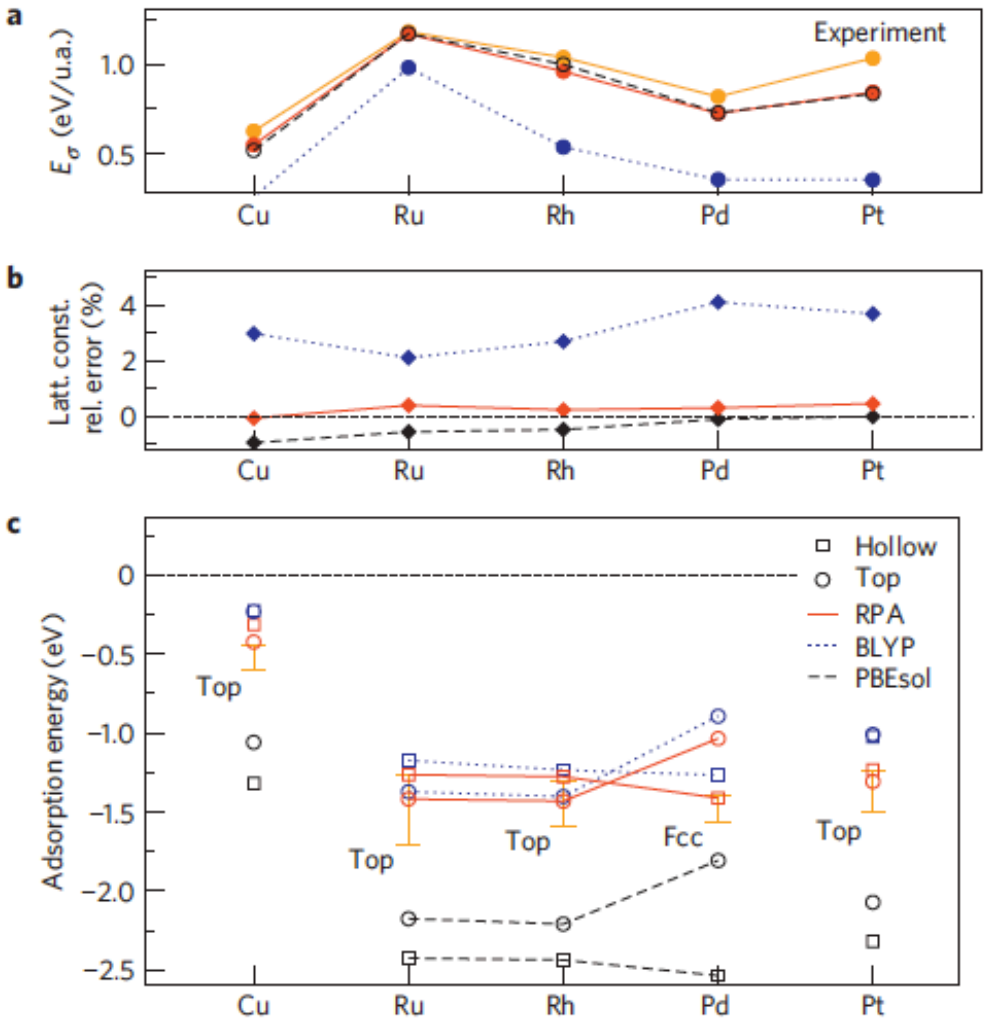


**Figure 3 | Surface energies, lattice constants and adsorption energies.** **a**, Fcc(111) surface energies ($E_\sigma$) for PBEsol, BLYP and RPA. Experimental surface energies are deduced from liquid-metal data[24,25]. **b**, Lattice constants for PBEsol, RPA and BLYP. **c**, Adsorption energies for the atop and hollow sites of CO on Cu, late 4*d* metals and Pt for PBEsol, RPA and BLYP. Experimental data with error bars are from ref. 26. The error bars correspond to the spread of the experimental results.

Schimka et al., Nature Materials 9, 741 (2010)

# Cubic scaling RPA

As shown by Adler and Wiser, the IP polarizability $\chi^0$ can be straightforwardly calculated from $\{\psi, \epsilon\}$:

$$\chi^0_{\mathbf{G},\mathbf{G}'}(\mathbf{q},\omega) = \frac{1}{\Omega}\sum_{nn'\mathbf{k}} 2w_{\mathbf{k}}(f_{n'\mathbf{k}+\mathbf{q}} - f_{n'\mathbf{k}}) \times \frac{\langle\psi_{n'\mathbf{k}+\mathbf{q}}|e^{i(\mathbf{q}+\mathbf{G})\mathbf{r}}|\psi_{n\mathbf{k}}\rangle\langle\psi_{n\mathbf{k}}|e^{-i(\mathbf{q}+\mathbf{G}')\mathbf{r}'}|\psi_{n'\mathbf{k}+\mathbf{q}}\rangle}{\epsilon_{n'\mathbf{k}+\mathbf{q}} - \epsilon_{n\mathbf{k}} - \omega - i\eta}$$

Expensive: this scales as $N^4$!

# Cubic-scaling RPA

M. Kaltak, J. Klimeš, and G. Kresse, PRB 90, 054115 (2014)

Evaluate the Green's function in "imaginary" time:

$$G(\mathbf{r},\mathbf{r}',i\tau) = \sum_n \psi_n(\mathbf{r})\psi_n^*(\mathbf{r}')e^{-\epsilon_n\tau}$$

and the polarizability as:

$$\chi^0(\mathbf{r},\mathbf{r}',i\tau) = -G(\mathbf{r},\mathbf{r}',i\tau)G(\mathbf{r},\mathbf{r}',-i\tau)$$

Followed by a cosine-transform:

$$\chi^0(\mathbf{r},\mathbf{r}',i\tau) \xrightarrow{\text{CT}} \chi^0(\mathbf{r},\mathbf{r}',i\omega)$$

Now the worst scaling steps are the evaluation of the Greens function ($N^3$), and

$$E_c = \int_0^\infty \frac{d\omega}{2\pi}\text{Tr}\{\ln[1-\chi_0(i\omega)\nu] + \chi_0(i\omega)\nu\}$$

(which scales as $N^3$ due to the diagonalization involved in evaluating the "ln").

The evaluation of the polarizability scales quadratically ($N^2$)!

But storing G and χ is expensive! → we need small sets of cleverly chosen "τ" and "ω"

# The “minimax” fit

Express a function $f(x)$ in a basis of *N* functions $\{\varphi(\alpha_i, x)|i = 1, \dots, N\}$, such that the error:

$$\eta(\vec{\alpha}, \vec{\beta}, x) = f(x) - \sum_i \beta_i \varphi(\alpha_i, x)$$

is “as small as possible”.

Choose $\{(\alpha_i, \beta_i)|i = 1, \dots, N\}$ so that the *maximum error*:

$$||\eta||_\infty := \max_{a \leq x \leq b} |\eta(\vec{\alpha}, \vec{\beta}, x)|$$

is minimized.

This solution, $\{(\alpha_i^*, \beta_i^*)|i = 1, \dots, N\}$, is the so-called ”minimax” solution

# The “minimax” frequency grid

M. Kaltak, J. Klimeš, and G. Kresse, JCTC 10, 2498 (2014)

The IP polarizability can be written as (Adler&Wiser):

$$\chi(i\omega) = \sum_{\mu} \chi_{\mu}\phi(\omega, x_{\mu}) \qquad \chi_{\mu(=ia)} = \langle i|\mathbf{r}|a\rangle\langle a|\mathbf{r}'|i\rangle \qquad x_{\mu(=ia)} = \epsilon_a - \epsilon_i$$

where $\phi(\omega, x) = \dfrac{2x}{x^2 + \omega^2}$

Determine a frequency grid and quadrature weights by expressing the “2nd-order direct Møller-Plesset energy”

$$E_c^{(2)} = -\frac{1}{8\pi}\int_{-\infty}^{\infty} d\omega\{\chi(i\omega)\nu\}^2$$

in the basis $\{\phi(\omega_i, x)|i = 1, \ldots, N\}$ in the minimax sense:

$$\{(\gamma_k^*, \omega_k^*)|k = 1, .., N\} \qquad \eta(\vec{\gamma}, \vec{\omega}, x) = \frac{1}{x} - \frac{1}{\pi}\sum_{k=1}^{N}\gamma_k\phi^2(\omega_k, x) \qquad E_g \leq x \leq \max(\epsilon_a - \epsilon_i)$$

$$E_c^{(2)} = -\frac{1}{8\pi}\int_{-\infty}^{\infty} d\omega\{\chi(i\omega)\nu\}^2 \longrightarrow E_c^{(2)} \approx -\frac{1}{8\pi}\sum_{k=1}^{N}\gamma_k^*\{\chi(i\omega_k^*)\nu\}^2$$

# The “minimax” time grid

## M. Kaltak, J. Klimeš, and G. Kresse, JCTC 10, 2498 (2014)

Alternatively the IP polarizability can be written as:

$$\hat{\chi}(i\tau) = \sum_{\mu} \chi_{\mu} \hat{\phi}(\tau, x_{\mu}) \qquad \chi_{\mu(=ia)} = \langle i|\mathbf{r}|a\rangle\langle a|\mathbf{r}'|i\rangle \qquad x_{\mu(=ia)} = \epsilon_a - \epsilon_i$$

where $\hat{\phi}(\tau, x) = e^{-x|\tau|}$

Determine a frequency grid and quadrature weights by expressing the “2nd-order direct Møller-Plesset energy”

$$E_c^{(2)} = -\frac{1}{4}\int_{-\infty}^{\infty} d\tau \{\hat{\chi}(i\tau)\nu\}^2$$

in the basis $\left\{\hat{\phi}(\tau_i, x)\middle| i = 1, \ldots, N\right\}$ in the minimax sense:

$$\{(\sigma_k^*, \tau_k^*)|k = 1, .., N\} \qquad \hat{\eta}(\vec{\sigma}, \vec{\tau}, x) = \frac{1}{2x} - \sum_{k=1}^{N} \sigma_k \hat{\phi}^2(\tau_k, x) \qquad E_g \leq x \leq \max(\epsilon_a - \epsilon_i)$$

$$E_c^{(2)} = -\frac{1}{8\pi}\int_{-\infty}^{\infty} d\omega \{\chi(i\omega)\nu\}^2 \longrightarrow E_c^{(2)} \approx -\frac{1}{4}\sum_{k=1}^{N} \sigma_k^* \{\hat{\chi}(i\tau_k^*)\nu\}^2$$

# The non-uniform cosine transform

M. Kaltak, J. Klimeš, and G. Kresse, JCTC 10, 2498 (2014)

The cosine transform of $\chi(i\omega) \leftrightarrow \chi(i\tau)$:

$$\chi(i\omega) = 2\int_0^\infty d\tau \hat{\chi}(i\tau)\cos(\omega\tau) \qquad \hat{\chi}(i\tau) = \frac{1}{\pi}\int_0^\infty d\omega \chi(i\omega)\cos(\omega\tau)$$

is reformulated on the minimax frequency and time grids as

$$\chi(i\omega_k) = \sum_{l=1}^{N} a_{kl}\hat{\chi}(i\tau_l) \qquad a_{kl} = w_{kl}\cos(\omega_k^*\tau_l^*)$$

where the coefficients $w_{kl}$ are the minimax solution to the following fitting problem:

$$\eta^c(\vec{w}_k, x) = \phi(\omega_k^*, x) - \sum_{l=1}^{N} w_{kl}\cos(\omega_k^*\tau_l^*)\hat{\phi}(\tau_l^*, x) \xrightarrow{\text{minimax fit}} \{w_{kl}^* | k, l = 1, .., N\}$$

for fixed $\{\omega_k^*\}$ and $\{\tau_k^*\}$, and for $E_g \leq x \leq \max(\epsilon_a - \epsilon_i)$.

# How good are the grids: ZnO and Si

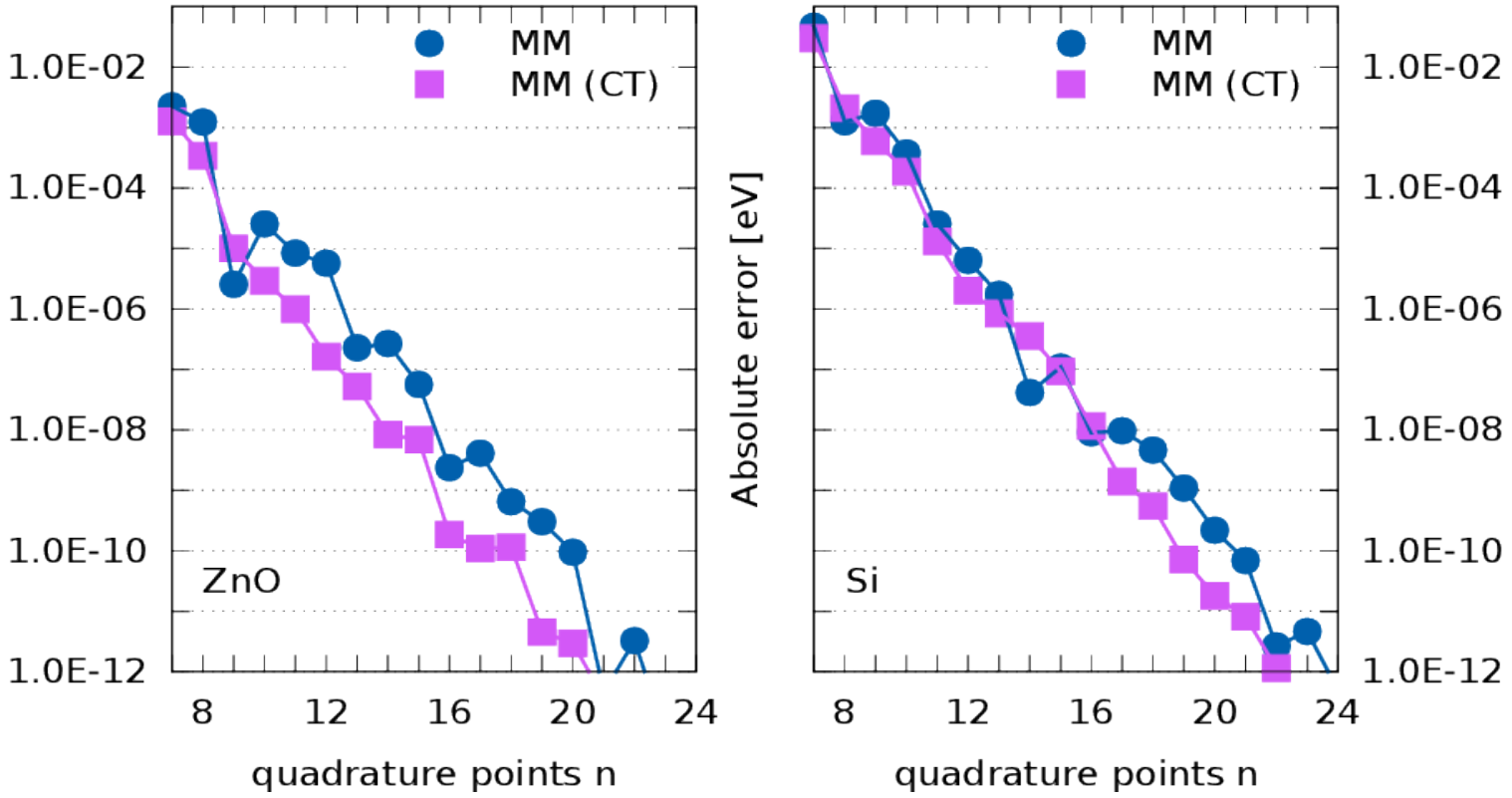


- $N^4$ RPA calculations entirely in frequency
- $N^2$ calculation of polarizability in time, then transformation to frequency (200 atoms on 200 cores in about one hour)

M. Kaltak, J. Klimeš, and G. Kresse, JCTC 10, 2498 (2014); PRB 90, 054115 (2014).

# Scaling

New RPA code (VASP6):

- Scales linearly in the number of k-points (as DFT), instead of quadratically as for conventional RPA and hybrid functionals
- Scales cubically in system size (as DFT).

Prefactors are much larger than in DFT, but calculations for 200 atoms take less than 1 hour (128 cores)

Si defect calculations: 64-216 atoms

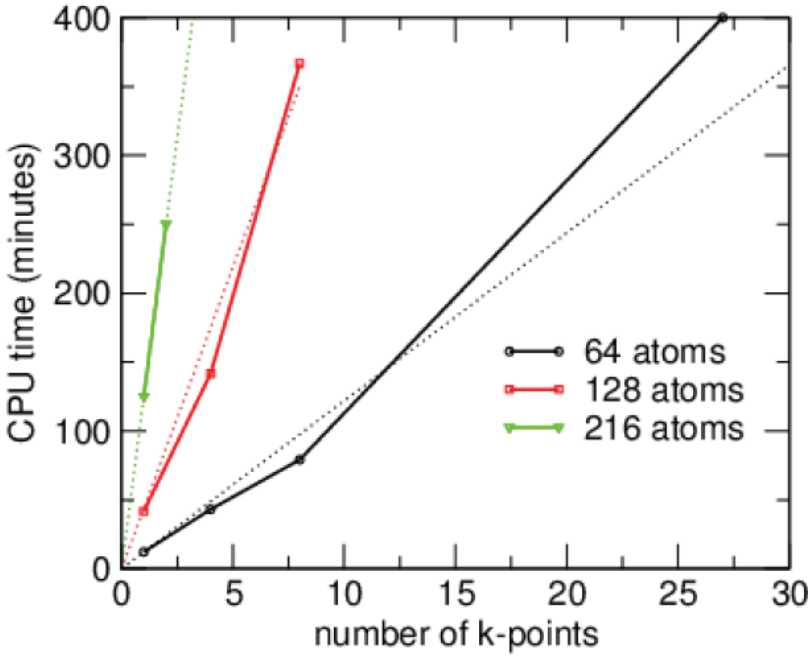


TABLE I. Timings in minutes for an RPA calculation for different bulk Si bcc cells. The calculations are done for the Γ point only and the number of cores is increased with system size. Since one of the computational steps scales only quadratically with system size, the total scaling is better than cubic.

| Atoms | Cores | Time | Time×cores/atoms$^3$ × $10^3$ |
|---|---|---|---|
| 54 | 32 | 14.3 | 2.91 |
| 128 | 64 | 83.2 | 2.54 |
| 250 | 128 | 299.9 | 2.45 |

# Defect formation energies in Si

| | PBE | HSE | HSE(+vdW) | QMC | RPA |
|---|---|---|---|---|---|
| Dumbbell X | 3.56 | 4.43 | 4.41 | 4.4(1) | 4.28 |
| Hollow H | 3.62 | 4.49 | 4.40 | 4.7(1) | 4.44 |
| Tetragonal T | 3.79 | 4.74 | 4.51 | 5.1(1) | 4.93 |
| Vacancy | 3.65 | 4.19 | 4.38 | | 4.40 |

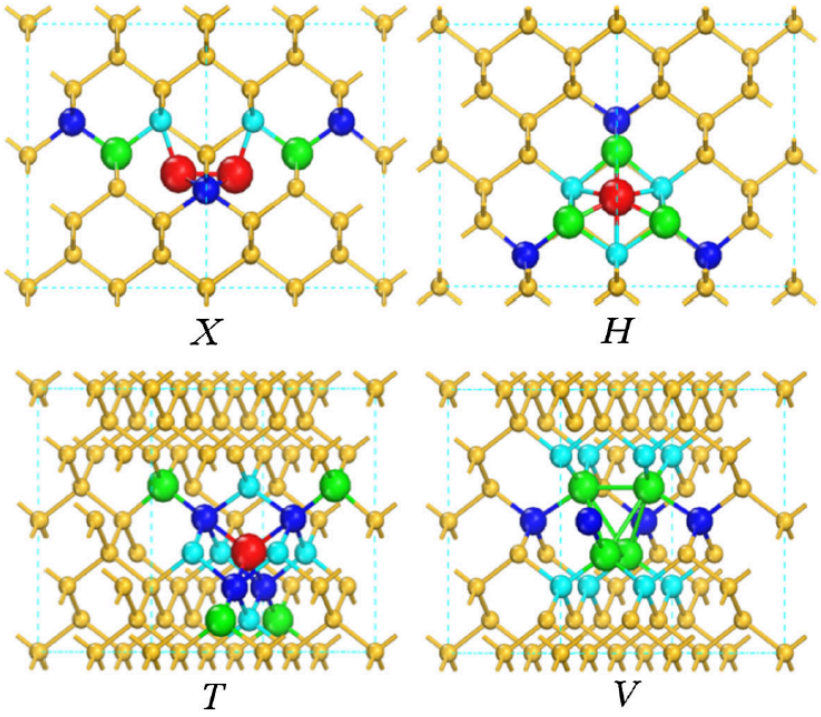


pictures and HSE+vdW:
Gao and Tkatchenko,
PRL 111, 045501 (2013).

QMC:
Parker, Wilkins, and Hennig,
Phys. Status Solidi B 248, 267 (2011).

# Cubic-Scaling GW

P. Liu, M. Kaltak, J. Klimeš, and G. Kresse, PRB 94, 165109 (2016)

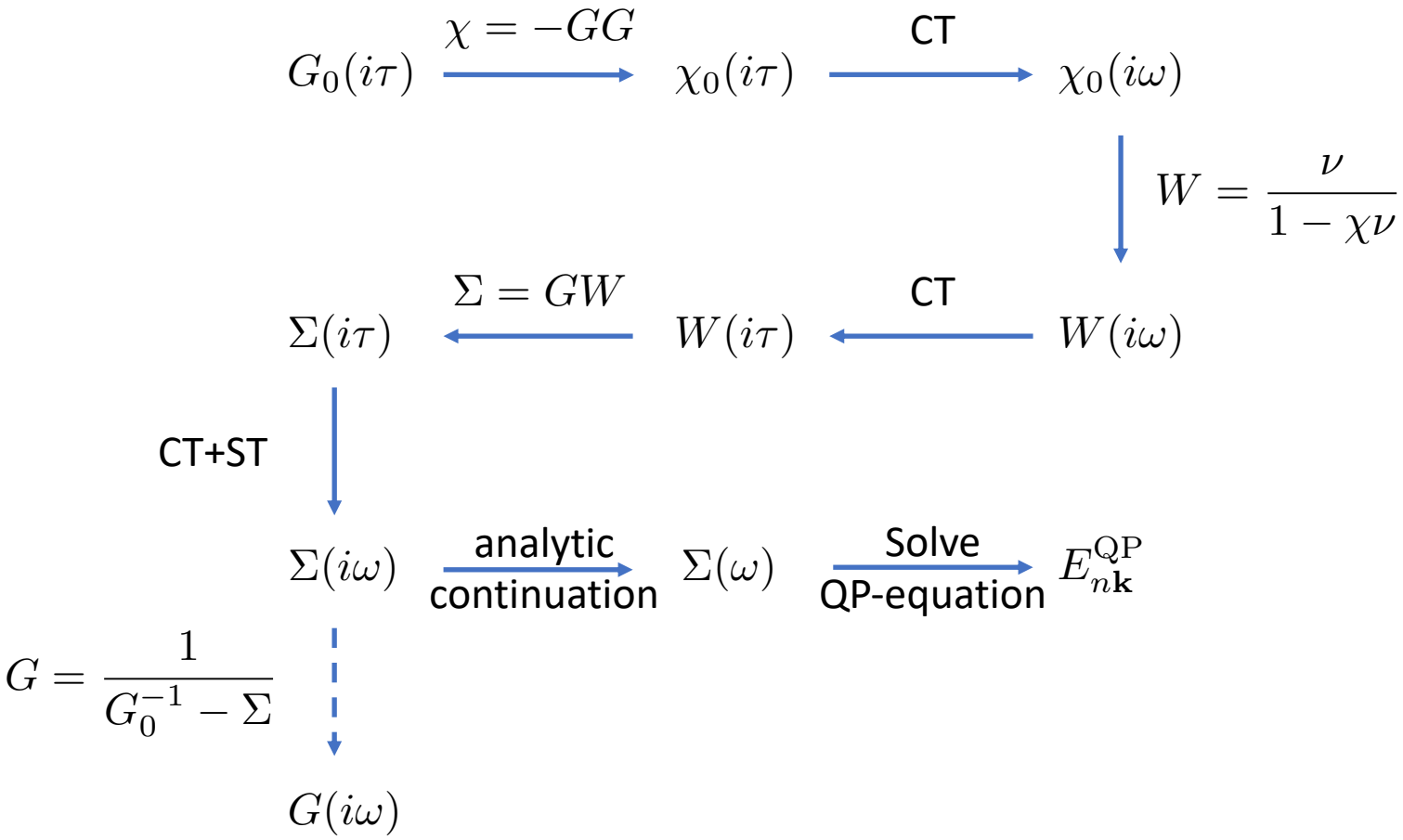

- Minimax grids:
  M. Kaltak, J. Klimeš, and G. Kresse, JCTC 10, 2498 (2014); PRB 90, 054115 (2014).

- Cubic-scaling RPA total energies (ACFDT):
  M. Kaltak, J. Klimeš, and G. Kresse, PRB 90, 054115 (2014).

- Cubic-scaling RPA quasi-particles (GW):
  P. Liu, M. Kaltak, J. Klimeš, and G. Kresse, PRB 94, 15109 (2016).

- Finite temperature grids (!):
  M. Kaltak and G. Kresse, PRB 101, 205145 (2020)

Dr. Merzuk Kaltak
(VASP Software GmbH)

# Forces in the RPA

$$\frac{\partial E}{\partial R} = \langle\psi|\frac{\partial H}{\partial R}|\psi\rangle + \langle\frac{\partial \psi}{\partial R}|H|\psi\rangle + \langle\psi|H|\frac{\partial \psi}{\partial R}\rangle$$

Non-Hellmann-Feynman!

Hellmann-Feynman theorem: when the orbitals are eigenstates of the Hamiltonian, the second and third terms on the RHS are zero.

In the RPA we need to consider ”non-Hellmann-Feynman” contributions!

These take the following form:

“from linear response”

$$\langle\frac{\partial \psi}{\partial R}|H|\psi\rangle + \langle\psi|H|\frac{\partial \psi}{\partial R}\rangle \longrightarrow \left(\int G_0(i\omega)\,\frac{\partial E_{\mathrm{RPA}}}{\partial G}\bigg|_{i\omega} G_0(i\omega)d\omega\right)\frac{\partial V_{\mathrm{KS}}}{\partial R}$$

$$\frac{\partial E_{\mathrm{H}}}{\partial G} = V_{\mathrm{H}} \qquad \frac{\partial E_{\mathrm{X}}}{\partial G} = V_{\mathrm{X}} \qquad \frac{\partial E_{\mathrm{c}}}{\partial G} = \Sigma$$

# Forces in the RPA

A test: ”RPA forces” (lines) vs. energy derivatives from finite differences (symbols):

(Diamond 8 atom super cell)

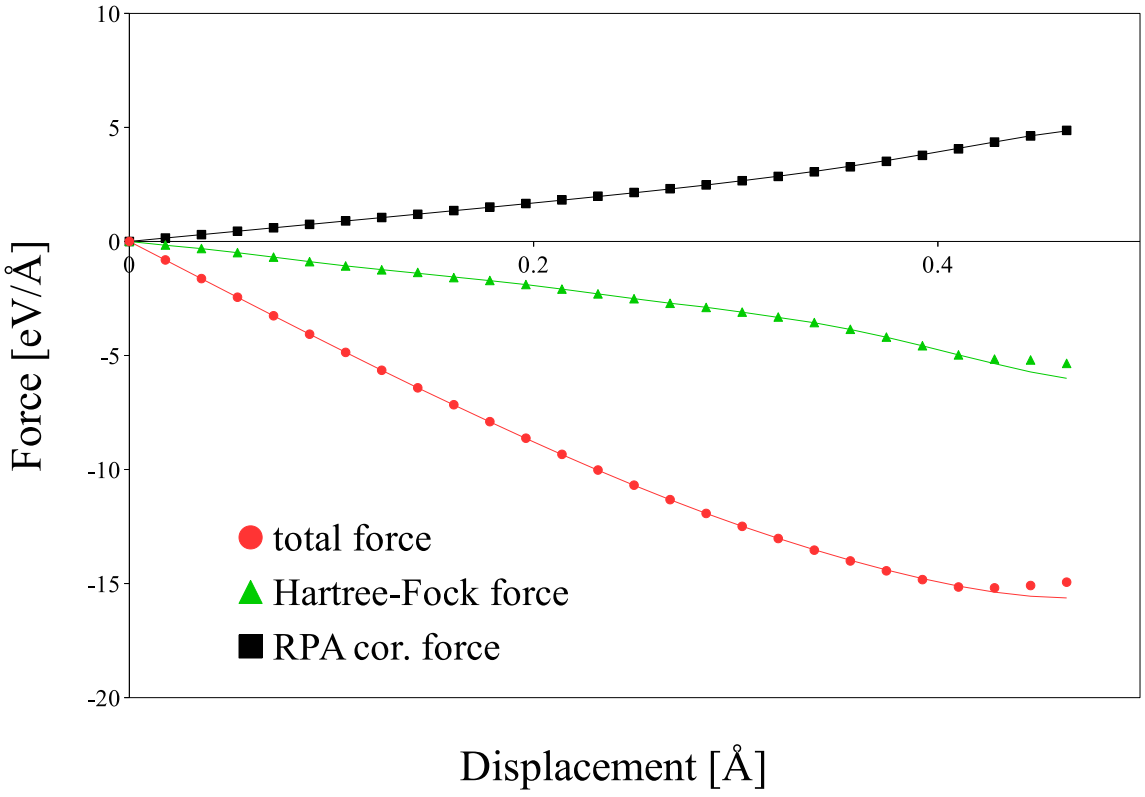

RPA Diamond (128 atom super cell) PBE

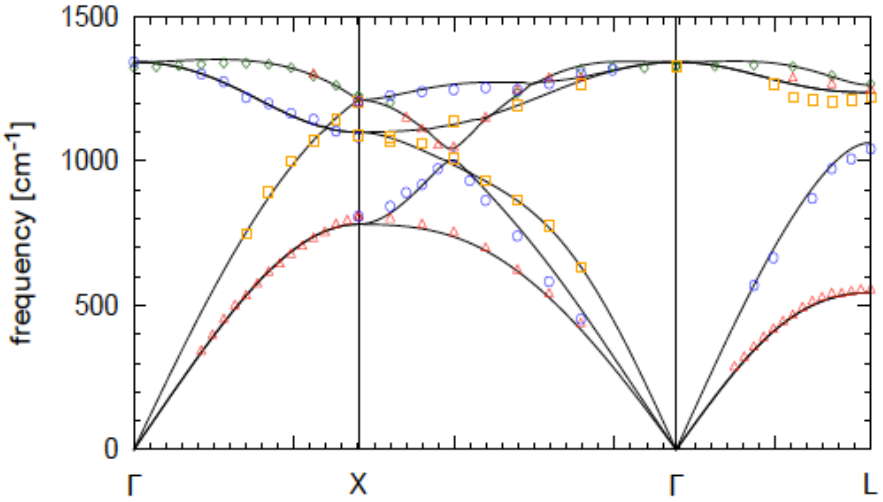


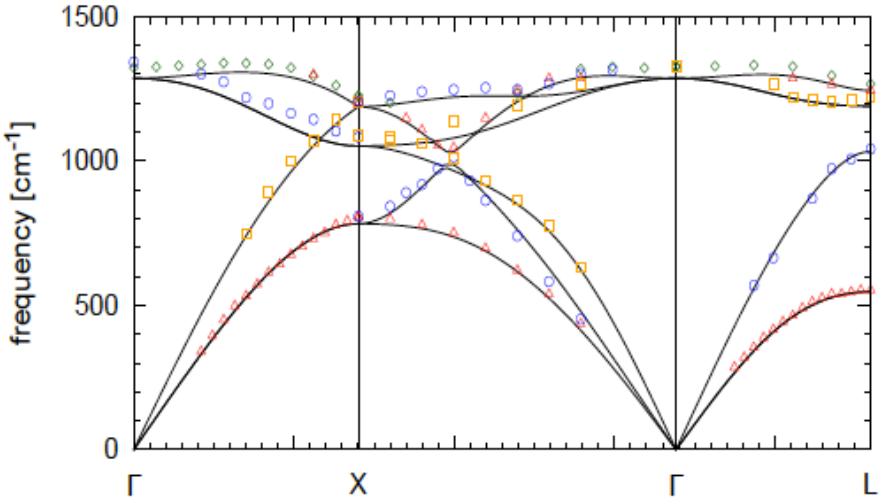


RPA Graphite (128 atom super cell) PBE

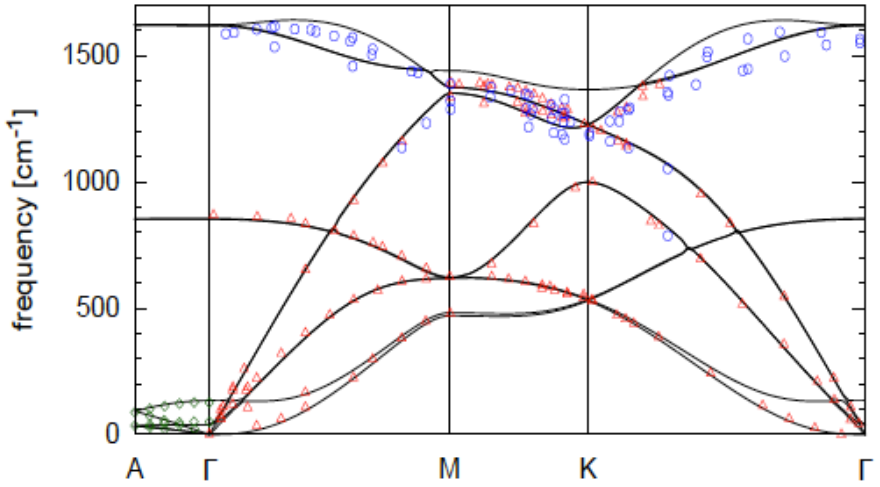


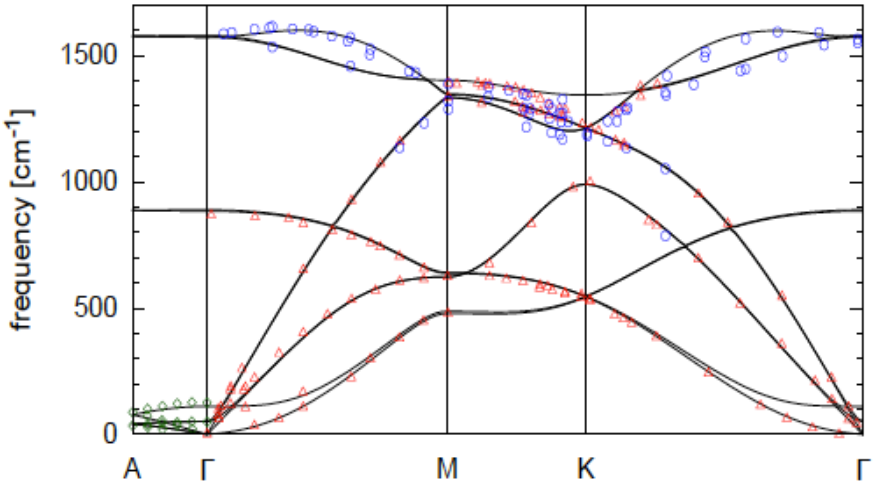

# Summary

- Beyond DFT: the RPA
  - Well balanced description of all bond types (metallic, covalent, ionic, vdW)
  - Unfortunately energy differences can still not be predicted with chemical accuracy
  - But at the moment the optimal balance between accuracy and computational effort
- Cubic-Scaling RPA
  - Both for total energies as well as for quasi-particles
  - Minimax frequency and time grids
  - Near future: finite temperature RPA
- Forces in the RPA

# Implementation in MedeA 3.1

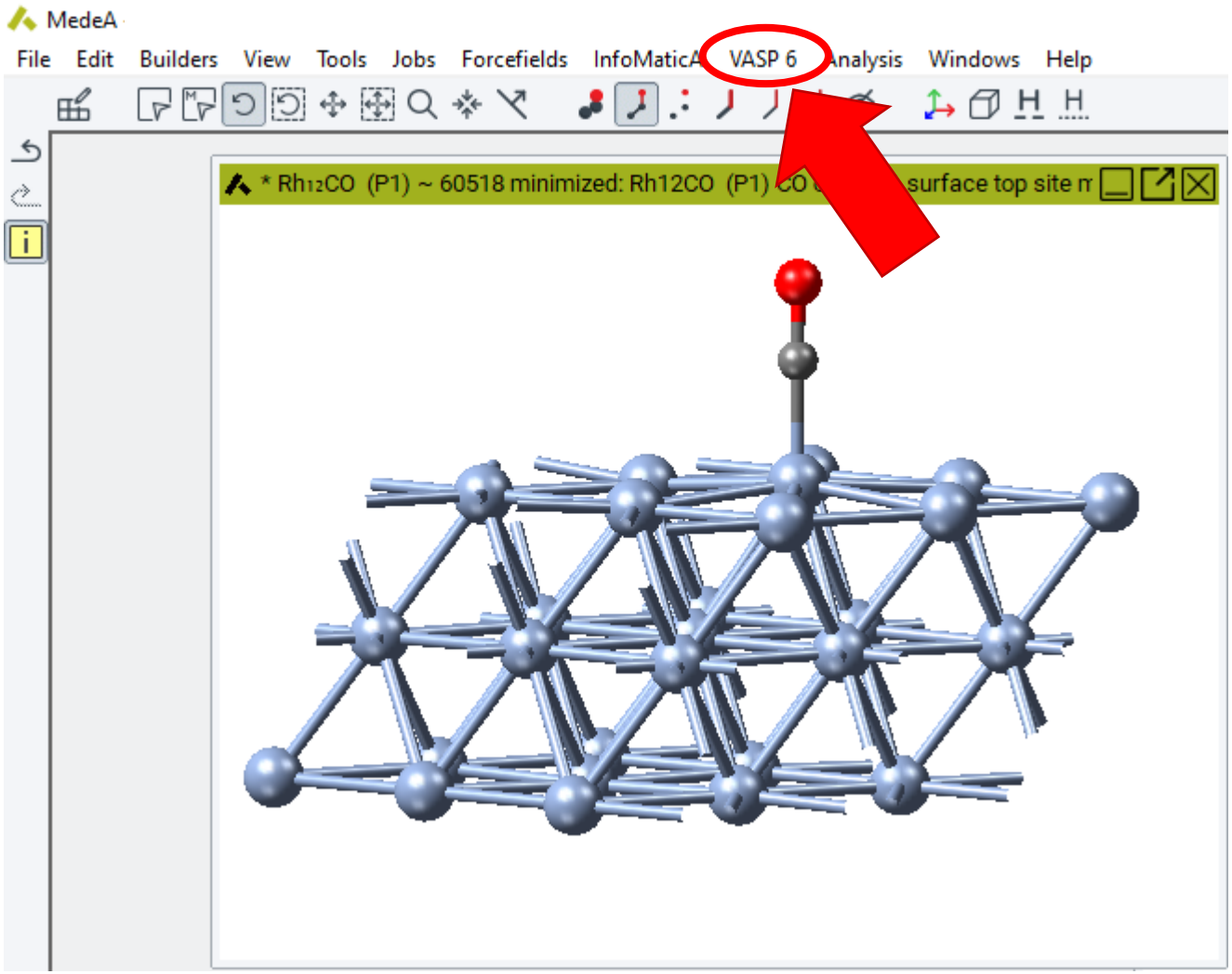

# Implementation in MedeA 3.1

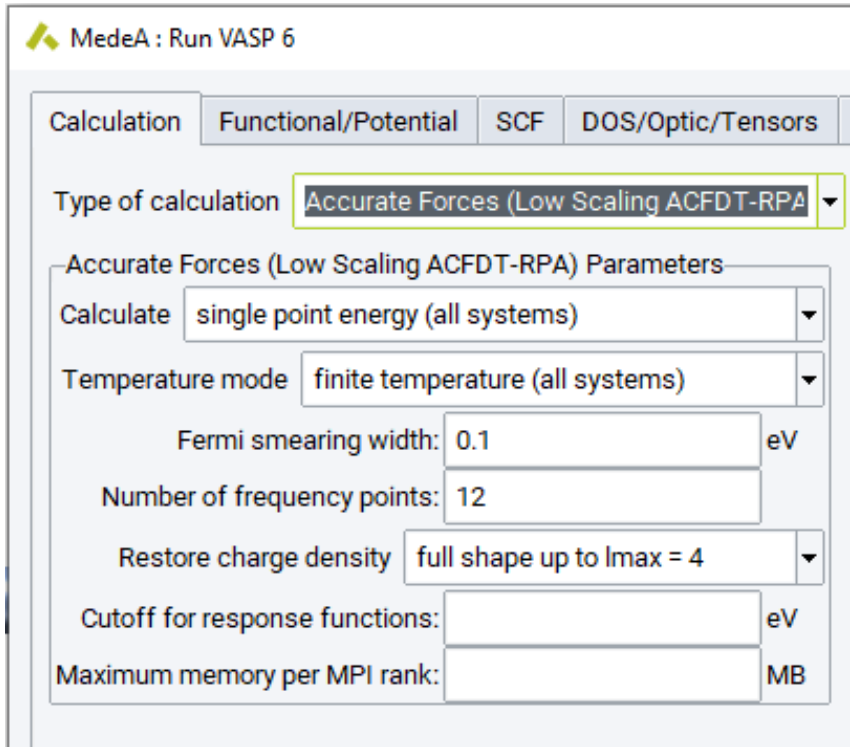

# Implementation in MedeA 3.1

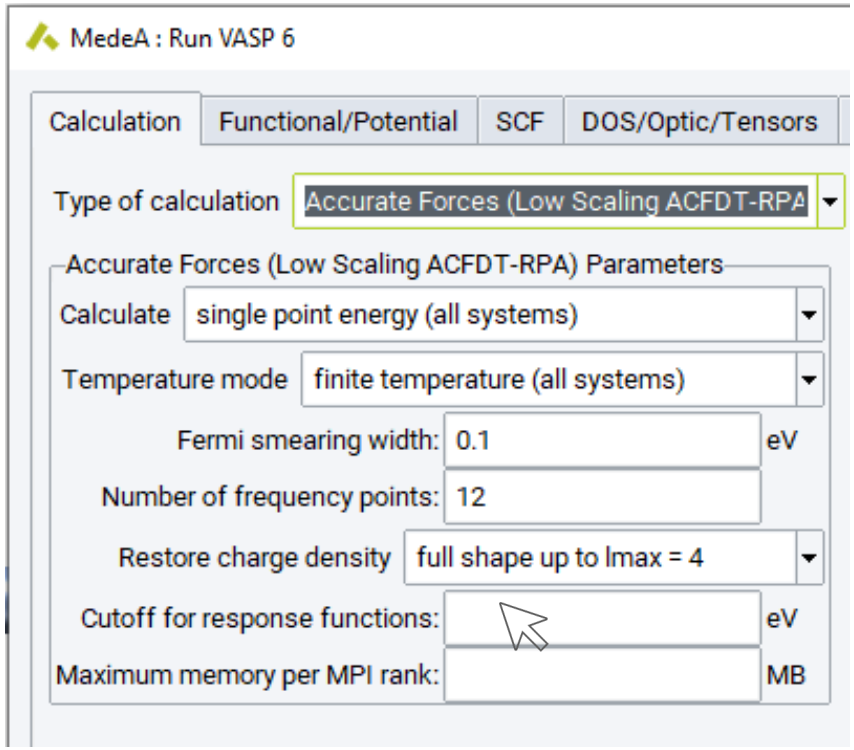

# Implementation in MedeA 3.1

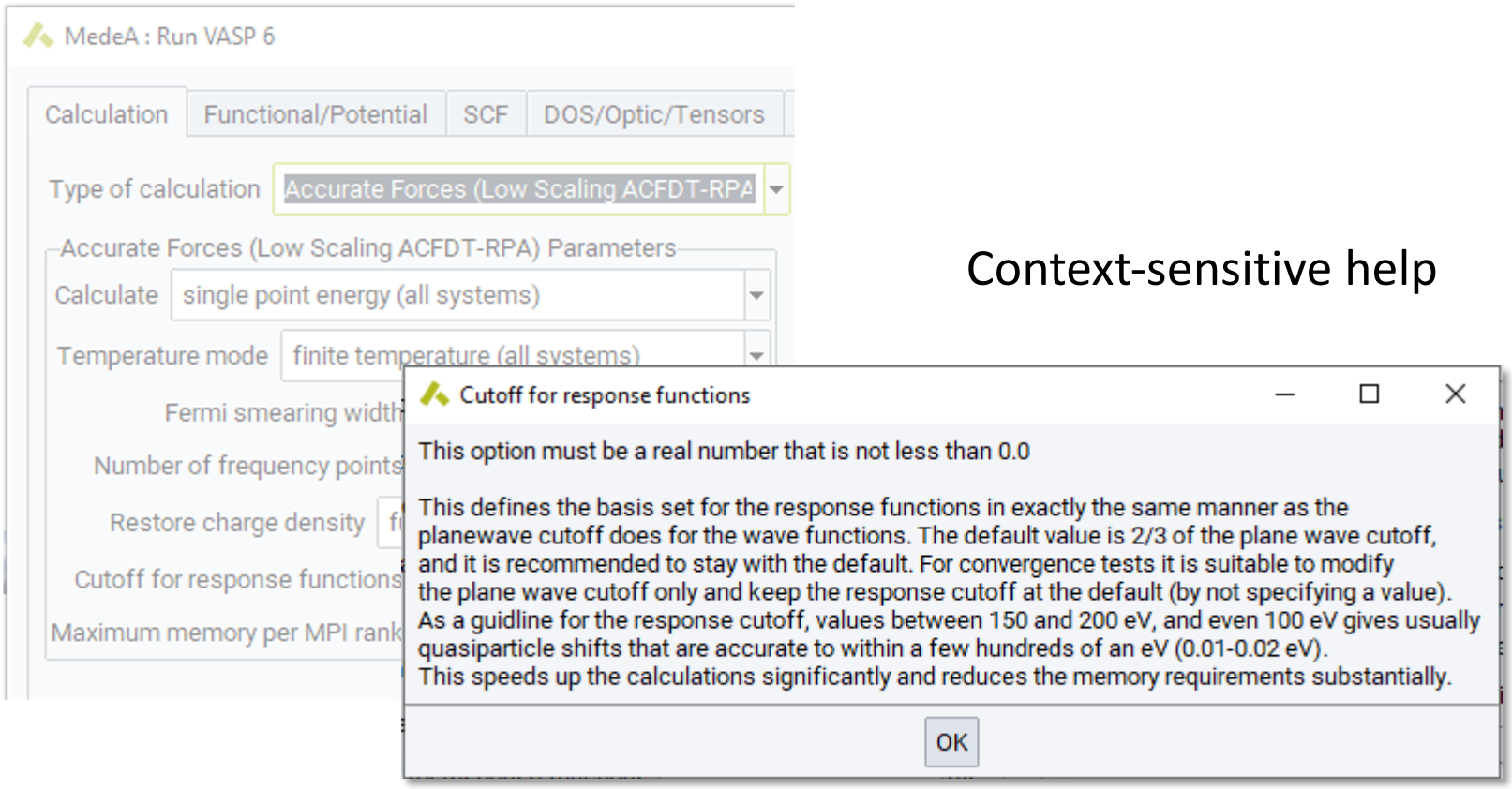


Context-sensitive help

# Implementation in MedeA 3.1

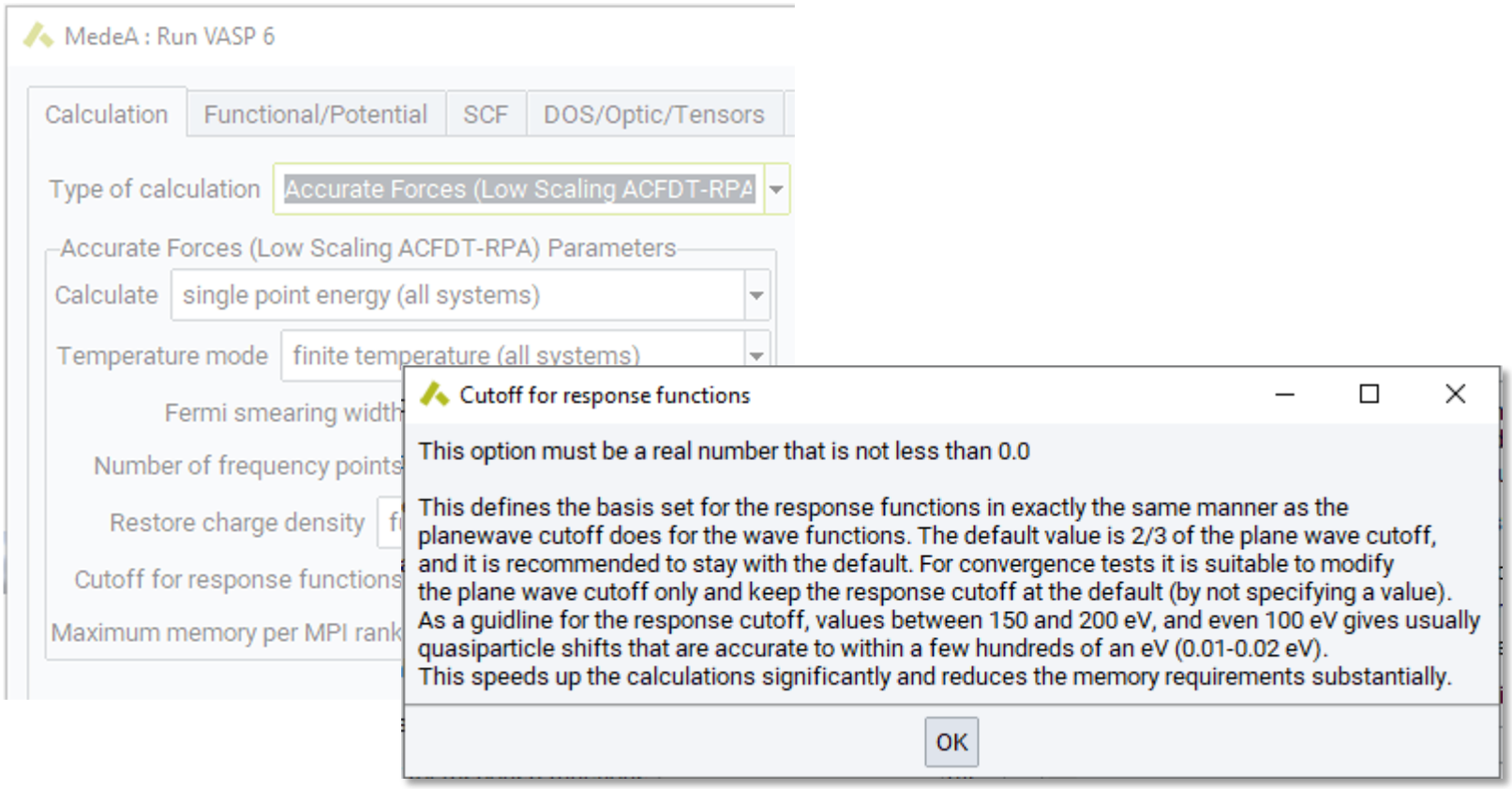


More in the upcoming Webinars

# The End

Thank you for your attention!

# Materials Design UGM

San Diego, California

Oct. 13 – 15

www.materialsdesign.com/ugm-2020

# *MedeA* 3.1 Webinars

June 2020: Elasticity and beyond – Predicting Mechanical Properties with *MedeA*, by Ray Shan

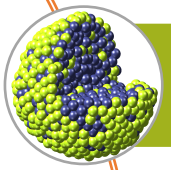

June 2020: Diffusion by Erich Wimmer and Benoît Minisini

July 2020: VASP 6 by Martjin Marsman

July 2020: Mesoscale modeling by Jörg-Rüdiger Hill

August 2020: *MedeA* 3.1 by Marianna, Walter and Jörg-Rüdiger Hill

Upcoming in the fall of 2020: Additional webinars addressing accuracy and larger scales

# Questions about the webinar

***Katherine Hollingsworth***

*khollingsworth@materialsdesign.com*

materials design

*info@materialsdesign.com*

*www.materialsdesign.com*

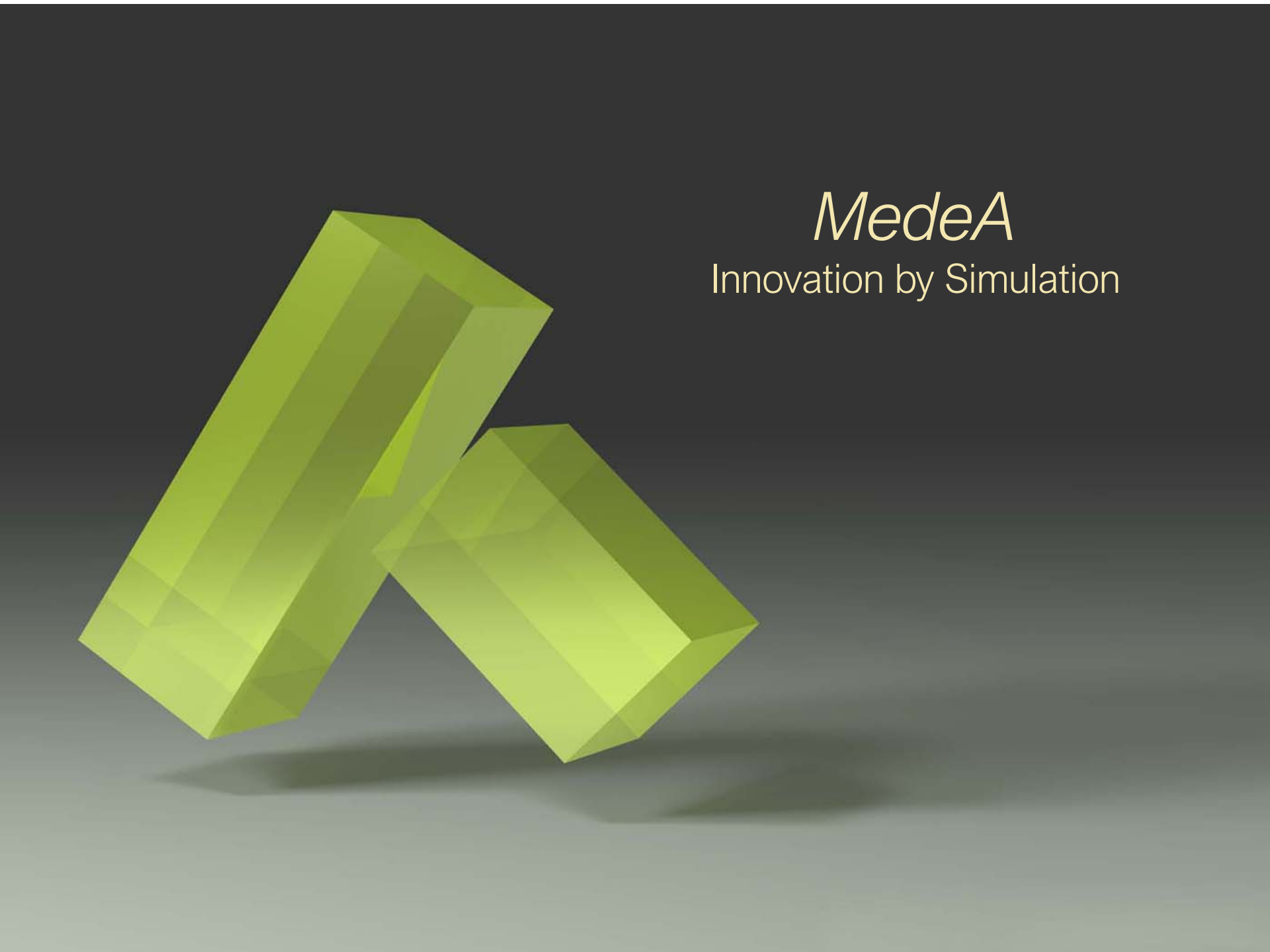
MedeA
Innovation by Simulation